

## **Acknowledgement**

I would like to thank those whom have contributed to the realization of my thesis, at first I would like to thank Prof. Abdelrahman Elzobair for his guidance and assistance and providing me all necessary guidelines and for his constant supervision through the progress of this work and helping in all the aspects of my research.

This work would not have been possible without the help and support of my husband and his patience and encouragement throughout the period of this research and giving me a power to finish thesis, to him deep gratitude and thanks.

I would like to thank the family of the Civil Engineering Department of Sudan University of Science & Technology (SUST).

Finally I would like to express my deep gratitude to my loving parents, my siblings, my children and all my friends whose love ,care, always encourage and support me.

## ABSTRACT

**Piles** offer an innovative alternative for foundations in expansive soils; Driven piles, in particular have been a preferred foundation system because of their relative ease of installation and low cost .There are some phenomena like heave or settlement that occur in the soil related with the process of driving pile in expansive soil.

This research presents a numerical model of driven piles in expansive soil using the finite element program PLAXIS 2D. The dynamic analysis was performed to investigate the effects of driving process in the pile and the adjacent soil. Four documented cases are considered to validate the numerical model. The first case is Demonstration Example for driven pile, whereas the other three are case studies in some locations in Khartoum city which represented the expansive soil. The results of the study showed the presence of some phenomena associated with the effects of vibration due to process of driving pile in the expansive soil, like settlement of the soil surrounding the pile and the heave of driven pile which can be controlled by a certain procedure before the process of the driving pile to avoid or minimize the effects, the pile may be driven in a predrilled hole or jetted or jacked into place.

Also the influence of the length of the pile on these phenomena was studied and it found that the length of pile make a significant factor for these phenomena because the increase of pile length increases the heave of pile and the settlement of the soil surrounding the pile in the expansive soil.

## المستخلص

تمثل الاوتاد بديلا مبتكرا للاساسات في التربة المنتفخة نتيجة لتعرضها للماء وتعتبر الاوتاد المغروزة عن طريق الدق نوعا مفضلا من انواع الاوتاد وذلك لسهولة تركيبها وقلة تكلفتها وملائمتها للمناطق التي يصعب فيها تنفيذ الاوتاد المصبوبة في الموقع .هناك بعض الظواهر المرتبطة بالاهتزازات المتولده نتيجة لدق الاوتاد في التربه المنتفخه مثل الهبوط والانتفاخ الذي يحدث في التربة المحيطة بالوتد وايضا ارتداد الوتدأو ارتفاعه والذي قد يتسبب في بعض المشاكل في المنشآت القريبة من منطقة الغرز.

يقدم هذا البحث نموذج عددي لاوتاد مغروزه في تربه منتفخه ومن ثم عمل نماذج عددية وتحليلها باستخدام برنامج العناصرالمحدده منها نماذج تمثل دراسات حالة لمواقع مختلفة في منطقة الخرطوم تعتبر مثالا للتربة المنتفخة ، تم اجراء التحليل الديناميكي للتحقيق في الآثار المترتبة علي العمليه الديناميكية لدق الخازوق علي التربه المحيطة به وايضا علي الخازوق نفسه . تم عمل أربعة نماذج النموذج الأول عباره عن مثال لتوضيح كيفية إستخدام البرنامج ،بينما النماذج الثلاثه الأخرى تمثل دراسات حالة لثلاثة مواقع مختلفة في مدينه الخرطوم والتي تعتبر مثالا للتربة المنتفخه . أظهرت نتائج الدراسة وجود بعض الظواهر المرتبطة بعملية الدق في التربه الطينية كهبوط التربة المحيطة بالخازوق والتي قد تمثل مشكلة في بعض الأحيان ولكن يمكن التحكم فيها باتباع بعض الاجراءات قبل عملية الدق مثل الحفر بالمتقاب الدوار إلي عمق معين وبعض الاجراءات الأخرى التي ضمنت في هذا البحث.

أيضا اجريت دراسه لتأثير طول الوتد علي هذه الظواهر المرتبطة بدق الاوتاد في التربه المنتفخه وبينت الدراسه ان طول الخازوق يعتبر عاملا مهما في زيادة هبوط التربه المحيطة بالخازوق وكذلك في ارتفاع الوتد او ارتداده لانه بزيادة طول الوتد يزيد ارتداد الوتد وايضا يزيد الهبوط في التربة المحيطة بالوتد في ظل وجود هذه الظواهر.

# Contents

<b>Content.....</b>	<b>Page No</b>
Acknowledgement.....	I
ABSTRACT.....	II
Table of Content.....	IV
List of Figures.....	VIII
List of table.....	X
Notations.....	XI
 <b>Chapter one Introduction</b>	
1.1 Background.....	1
1.2 Problem statement.....	2
1.3 Research Questions .....	2
1.4 Objectives.....	3
1.5 Methodology.....	3
1.6 Thesis layout.....	4
 <b>Chapter two Literature review</b>	
2.1 Introduction .....	6
2.2 Previous studies.....	6
2.3 Finite Element Method (FEM).....	11
2.4 General Information of PLAXIS 2D.....	12
2.4.1 Elements.....	13
2.4.2 Interface element.....	15
2.4.3 Analysis types.....	16
2.4.4 Material models.....	17

2.5 Pile foundation.....	19
2.5.1 The methods of inserted Piles into the soil.....	21
2.6 Some phenomena in expansive caused by driving process.....	22
2.6.1Pile Heave.....	23
2.6.2 Procedure to control eave.....	24
2.6.3Settlements.....	24
2.6.4 Immediate Settlement.....	25
2.6.5 Consolidation Settlement.....	25
2.6.6 Secondary Compression Settlement.....	25
2.6.7 Distortion Settlement.....	26
2.6.8 Procedure to control settlement.....	26

### **Chapter three Theoretical background**

3.1Introduction.....	27
3.2 Basic Equation Dynamic Behavior.....	27
3.3 Time Integration.....	28
3.3.1 Critical Time Step.....	30
3.3.2 Wave Velocity.....	31
3.4 Model Boundaries .....	32
3.5 Viscous Boundaries.....	33
3.6 Initial Stresses and Stress Increments.....	34
3.7 Linear Elastic-Perfectly Plastic Model.....	35
3.7.1 Linear Elastic Perfectly-Plastic Behavior.....	35
3.7.2 Formulation of the Mohr-Coulomb Model.....	37
3.7.3 Basic Parameters of the Mohr-Coulomb Model.....	40
3.7.4 Young's modulus (E).....	41
3.7.5 Poisson's ratio ( $\nu$ ).....	43

3.7.6 Cohesion (c).....	43
3.7.7 Friction angle ( $\phi$ ).....	43
3.7.8 Dilatancy angle ( $\psi$ ).....	44
3.7.9 Shear modulus (G).....	44
3.7.10 Odometer modulus ( $E_{oed}$ ).....	44
3.8 Advanced Parameters of Mohr-Coulomb model.....	45
3.8.1 Increase of stiffness (Increment).....	45
3.8.2 Increase of cohesion (increment).....	46
3.8.3 Tension cut-ff.....	46
3.9 Drainage type.....	46
3.9.1 Drained Behavior.....	47
3.9.2 Undrained behavior.....	47
3.9.3 Non-Porous Behavior.....	48
3.10 Dynamic Model arameters.....	48
3.10.1 Rayleigh alpha and beta.....	49
3.10.2 Determination of the Rayleigh damping coefficients.....	50
3.11 Water Conditions.....	51

## **Chapter four Piles in Modeling Expansive Soil Using PLAXIS2D Program**

4.1 Introduction .....	52
4.2 FEA simulation for driving pile using PLAXIS2D.....	52
4.3 Building Geometry.....	53
4.3.1 Dynamic loads.....	55
4.3.2 Material Data Sets.....	56
4.4 Mesh Generation.....	62
4 .4.1 Initial Conditions.....	63

4.5 Performing Calculation.....	63
4.5.1 Phase One.....	63
4.5.2 Phase Two.....	64
4.5.3 Phase Three.....	64
3.6 Viewing Output Results.....	65

## **Chapter five Analysis and Discussion of Results**

5.1 Introduction .....	68
5.2 Demonstrated example for driven Pile.....	68
5.3 The pile in White Nile bridge Area.....	70
5.4 The Pile of the Tuti Island bridge area.....	74
5.5 Comparison with different length of driven pile.....	76
5.6 The Pile of Khartoum Air Port area.....	78

## **Chapter Six Conclusion and Recommendation**

6.1 Introduction.....	79
6.2 Conclusions .....	79
6.3 Recommendations.....	80

<b>References.....</b>	<b>81</b>
------------------------	-----------

## **Appendices**

Appendix 1.....	84
Appendix 2.....	85
Appendix 3.....	87
Appendix 4.....	89

## List of Figures

Figure 2.1 nodes and stress point in –elements. (Brinkgreve 2006) .....	14
Figure 2.2 Distribution of nodes and stress points.....	14
Figure 2.3 local numbering and positioning of nodes.....	15
Figure 2.4 Distribution of nodes and stress points in the interface element....	16
Figure: 2.5 typical pile configurations.....	21
Figure: 2.6 Schematics of several pile hammers.....	23
Figure: 3.1 basic idea of an elastic perfectly plastic model.....	36
Figure: 3.2 the Mohr coulomb yield surface in principle stress space (C=0)...	38
Figure: 3.3 Definition of E0 and E50 for standard drained triaxial test result...	42
Figure: 3.4 Stress circle at yield ;one touches coulomb envelope .....	44
Figure: 3.5 Elastic parameters in Mohr-Coulomb and linear elastic models.....	53
Figure: 4.1 Dimensions tab sheet of the General Settings window.....	54
Figure: 4.2 Project tab sheet of the General Settings window.....	55
Figure: 4.3 main window of input program .....	58
Figure: 4.4 General tab sheet of the soil and interfaces data set window.....	57
Figure: 4.5 Geometry mode of pile driving .....	62
Figure: 4.6 Finite element mesh for driving pile .....	62



Figure: 4.7 Dynamic loading parameters .....	64
Figure: 4.8 the definition of the phases.....	65
Figure: 4.9 perform the calculation.....	66
Figure: 4.10 selection of phase from create animation window.....	67
Figure: 4.11 dynamic fields in curve generation window.....	67
Figure: 5.1 Pile settlement vs. time for General Example.....	69
Figure: 5.2 shows the shear stresses in the interface elements.....	69
Figure: 5.3 the deformed mesh of the last calculation phase.....	70
Figure: 5.4 the shear stresses in the interface elements.....	71
Figure: 5.5 the second calculation phase .....	71
Figure: 5.6 pile settlement vs. time for White Nile Bridge.....	72
Figure: 5.7 the deformed mesh of the last calculation phase.....	73
Figure: 5.8 the shear stresses in the interface elements.....	74
Figure: 5.9 shows the settlement of the pile for Tuti Island Bridge.....	75
Figure: 5.10 the deformed mesh of the last calculation phase.....	76
Figure: 5.11 the settlements due to driving pile with a different length.....	77
Figure: 5.12 the uplifted piles due to driving pile with a different length.....	77
Figure 5.13 the result of calculations of the phases of Khartoum airport.....	78

Figure: A.1 The Demonstration Example of pile driving situation.....	84
Figure: A.2 geometry model for the Demonstration Example of driven pile...	48
Figure: A.3 the output of the second calculation phase.....	86
Figure: A.4 General Information for the pile of White Nile bridge area.....	87
Figure: A.5 Load information for the pile of White Nile bridge area.....	87
Figure: A.6 Soil and Interface information for the pile of White Nile Bridge...	88
Figure: A.7 the displacement of the pile for of Khartoum airport.....	89
Figure: A.8 the deform mesh for of Khartoum airport.....	89

## List of tables

Table4:1 Soil and pile properties for the Demonstration example.....	58
Table4:2 Soil properties of White Nile Bridge (Al-Amery 2005).....	59
Table 4:3 Soil properties of Tuti island bridge (Al-Amery 2005).....	60
Table 4:4 Soil properties of Khartoum airport bridge (Al-Amery 2005).....	61
Table 5:1 The value of the settlements for the pile of White Nile Bridge .....	73
Table 5:2 the value of the heave for the pile and the soil of.....	75
Tuti Island Bridge area at selected nodes at surface	
Table 5:3 the value of the settlements and the heaves.....	76

## Notations

$\phi$ : Angle of internal friction

$\Psi$ : Angle of dilatancy

E: Young's Modulus of Elasticity

G: Shear Modulus

$\nu$ : Poisons Ratio

C: Cohesion

$\tau$ : Shear Stress

$\gamma$ : Unit weight Dry density of soil

$\lambda$  : Plastic multiplier

G : Shear modulus

$E_{ur}$ : The triaxial unloading stiffness

$E_{oed}$ : Odometer modulus

$V_p$  : Compression wave velocity

$V_s$ : Shear wave velocity

$\xi$  : Damping ratio

$R_{int}$ : Interface strength reduction factor

M: The mass matrix

$u$ : The displacement vector

$C$ : The damping matrix

$K$ : The stiffness matrix

$F$ : The load vector

$u$  : The displacement

$\dot{u}$  : The velocity

$\ddot{u}$ : The Acceleration:

$\alpha, \beta$ : The Rayleigh coefficients

# CHAPTER ONE

## INTRODUCTION

### 1.1 Background:

Expansive clay soils contain a significant component of expanding clay minerals, which undergo shrinking and swelling in response to drying and wetting.

The volume changes of expansive clay particles lead to volume changes of the soil mass, which are realized as vertical ground surface movements. This movement may cause some problems (e.g. Heave, settlement) with the founding of lightly loaded structures in many parts of the world.

Piles offer an innovative alternative for foundations in expansive clay soils. They are recommended in highly expansive soils and may be extending to large depths.

Pile can be classified up on:

- The effect on surrounding soils during installation (displacement, non-displacement); displacement piles are those which displace the soil to allow for the pile penetration.
- The material (concrete, reinforced concrete, wood and steel).
- The method of installation (bored, driven).

Driven piles, in particular, have been a preferred foundation system because of their relative ease of installation and low cost.

There are three main driving techniques to install driven piles and sheet as follows:

- Impact pile driving is known as the oldest technique of driving and produces a transient vibration in the ground, it is not preferred in urban areas and its use is more and more limited.
- Vibratory pile driving produces a harmonic vibration in the ground and is used to install piles in granular soils and with low operating frequency, also in cohesive soils.
- Jacking does not induce environmental disturbance but is very expensive. This technique is only used where sensitive environmental conditions are encountered

The vibratory pile driving technique has been preferred to other driving techniques due to economical, practical and environmental concerns.

## **1.2 Research Questions:**

Is the transmitted energy through the soil which was generated during the process of driving pile causes deformations in the pile and surrounded soil like settlement or heave or any other deformations?

## **1.3 Problem Statement:**

Analysis of driven pile foundations has typically been based on empirical and semi-empirical methods. Numerical methods offer an alternative solution to analyze pile foundation problems in a more comprehensive way. In this study, an investigation of numerical analysis of driven pile Foundation will be carried out.

The numerical modeling is going to be carried out by means of the Finite Element method as it allows for modeling complicated nonlinear soil behavior

and various interface conditions, with different geometries and soil properties. PLAXIS2D program will be used

## **1.4 Objectives:**

The aim of this research is

- To learn how to use the finite element method in modeling and analysis of driven piles
- To investigate the effects of vibrations and excess pore pressures resulting due to the driving process in the pile and surrounding soil
- To model and analyze the driven pile in expansive soil in many location in Khartoum area using the finite element program (PLAXIS2D )

## **1.5 Methodology:**

- In the first stage of this study, a comprehensive literature regarding the behavior of the piles in the expansive soil was collected and reviewed.
- In the second stage, the data was collected from two sources :The soil and pile properties for the Demonstration Example of driven piles to learn how to use PLAXIS2D finite element program is obtained from the PLAXIS2D tutorial manual in the web site of PLAXIS, and the soil properties for the case studies in different locations in Khartoum city in the Sudan were obtained from geotechnical investigations mainly performed by building and road research Institute and some other consulting firms(Al-Amery 2005 ).
- At the third stage, four models which represent the Demonstration Example of driven piles and the other three case studies were developed

to simulate the behavior of driven pile in expansive soil by using the finite element program PLAXIS2D Software

- At fourth stage the models were analyzed and the results which were obtained from the analysis were discussed. Finally the whole process was documented together with the important conclusions and recommendations for this study.

## **1.6 Thesis Layout:**

A brief explanation of each chapter is presented as follows:

- Chapter one: Presents a brief description of the expansive soil and types of pile foundation .it also contains brief description of the research problem, the objectives, the methodology which is be followed to carry out this study .Finally the thesis layout.
- Chapter two: States some studies about the behavior of pile foundation in the expansive soil, finite element method (FEM), general information about (PLAXIS2D) program, some problems in expansive soil related with the driving process and the procedure to control it.
- Chapter three: Outlines the finite element theory that used in PLAXIS2D for the dynamic calculation and analysis of driven piles.
- Chapter four: Presents the application of PLAXIS 2D. Also, it gives brief notes or guidelines for creation of model and simulation of the process of driven pile and the results output.



- Chapter five: Contains the output of the analysis and discussion of the results, also the comparison of the effects of the pile lengths is included in the discussions.
- Chapter six: Includes the conclusions of the research and some recommendations.

# **CHAPTER TWO**

## **LITERATURE REVIEW**

### **2.1 Introduction:**

In this chapter the literature regarding to driven piles foundation was given. Subsequently, the previous studies which is related with the driven piles, the finite element methods, information about PLAXIS2D, modeling of piles and soil, some problems related with driven process and the procedure to control these problems

### **2.2 Previous Studies:**

Studies into the pile foundation in expansive soils had proceeded in many directions and the behavior of the pile in the expansive soil had been studied by different methods, the following cases are examples for these studies:

Elbadawy et al (2001) Stated that Heave induced by expansive soils cause considerable damages and loses. And suggest that the Piles can effectively control heave in such soils. They used finite element program (ADINA) to study the effect of the pile length and the pile diameter on the pile heave. They concluded that the pile length is superior in decreasing the heave over the pile diameter and pile loading

Maki et al (2014) discussed the response behavior of pile foundation and seismic response analyses of RC pile-soil system were conducted using nonlinear finite element method. They clarifies that the deformation of the foundation was dramatically different in the dynamic analysis with that in the

static pushover analysis, interims especially of the location of the damage in the piles. In the results obtained by the 2-D models with different values of soil element thickness, macroscopic response at the top support was similar, whereas the damage level in the RC piles was remarkably different. The 2-D model in which the thickness of soil elements was equal to the footing width could give an equivalent result to the 3-D model. They conclude that the thickness of soil elements in 2-D finite element models should be carefully determined according to the effective width of the soil-structure interaction in each analytical target.

Jalali et al (2012) investigated the pile-soil interaction and its effect on the pile settlement and shear stress in the interaction zone. The impact of loading on the pile displacement was explored applying Mohr-Coulomb as well as Hard-soil behavior laws. they demonstrated that the Finite Element Analysis is an appropriate method to determine the effect of interface coefficient of pile and soil .also they stated that The Static Analysis of PLAXIS revealed that the pile settlement may be measured more accurately for the interface coefficients of (0.7 to 1) with Mohr - Coulomb behavior law of pile –soil compared to the Hard soil mode

Hekmat et al (2012) state that considering the fact that interaction of soil and pile when combined with effects of seismic loads are slightly complicated, this leads to utilize numerical analysis. The study, initially, attempts to provide a numerical solution for soil differential equation on pile-soil mechanism undergoing lateral loads by coupling finite element method and boundary element method. Therefore, the study discusses about soil parameters interchange in transfer function as well as displacement and cohesion. They concluded that shearing force at pile is very little and it gradually increases with

increase in depth. The maximum shearing force is imposed to the pile at its final part, while in approximately two third of pile length, the shearing force is zero. Also he concluded that the variation of the cohesion parameter has a considerable effect, since it causes yielding of several regions of the soil. They observed that in lower frequencies ( $0 < 0.45$ ) the response amplification in the case of plastic soil modeling is greater than the elastic condition. However, this difference is very small and negligible in higher frequencies.

Also he observed that transfer function has higher value when the separation effect between soil and pile is considered, but without considering that effect, the quantity is lower. Likewise, material's plastic feature has caused the maximum displacement and soil's plastic feature has given rise to a large value of a persistent displacement in soil. Moreover, non-linear characteristics of soil sometimes cause decrease or increase in seismic motions

Mhammedzein et al. (1999) developed a two dimensional axisymmetric finite element based model for analysis of soil-pile system in expansive soils. The pile was assumed to behave as linearly elastic while the soil was modeled as nonlinear elastic material. The pile was divided into 8-noded isoperimetric elements. The boundary conditions were the rollers on the left vertical face of the mesh were intended to simulate the condition of symmetry .complete contact between the soil and the pile was assumed at the soil-pile interface. The condition of a complete contact is considered appropriate for small movements ( $< 40\text{mm}$ ). Swelling and shrinking of the soil are related to change in soil are related to hang in soil suction. The predictions of the model were compared to the results of field experiments from two expansive soil sites in Sudan, Wad Mandeni and Elfao. The predictions of the numerical model were good agreement with filed results

The study shows that increases in pile length decrease the upward vertical movement of the pile. As the axial load increases, both the upward vertical movement and tensile stress decrease and eventually the pile may be subject only to downward movement and compresses for loaded piles occur throughout most portions of pile within the active zone with the maximum stress developing near the mid height of the pile

Al-Amery (2005) studied 24 sites in Khartoum city and found the ultimate vertical capacity for piles and, the results coupled with coordinate of the sites, where loaded into 3D pro beta v0.76 program for mapping contour lines for these result, so that we can find the weak and the strong areas in the studied region.

He concluded that the numerical model presented in his study for the analysis of soil-pile interaction gave very good results, but better results can be obtained if the following pointes are considered :-

The non-slip condition between pile and soil is used in the finite element analysis while the true condition is in between the no slip and full slip cases.

Interface element are needed to bridge the difference between the two material and two of the actual relative movement between pile and soil satisfy the physic The pile is subjected to high load that may lead to failure of pile; it is possible to improve his study by modeling piles as non-linear material

Masoumi and GDegrade(2005) presented a numerical model for the prediction of free field vibrations due to vibratory and impact pile driving. He stated that coupled FE-BE model had been developed to predict ground vibrations due to vibratory and impact pile driving. Using a sub domain formulation, a linear model for dynamic soil-pile interaction was implemented. The pile was modeled using the finite element method. The soil was modeled as a horizontally layered elastic half space using a boundary element method.

The characteristics of the propagating waves around the pile had been investigated. Induced waves classified into In the case of vibratory driving to the: vertically polarized shear waves around the shaft; the body waves around the pile toe, and the Rayleigh waves on the surface. Propagating waves due to impact driving were more complex. It was observed that deformations around the shaft were dominated by the vertically shear deformation where the normal and the radial deformations were small compared to shear deformations. In the far field, however, body waves were attenuated and Rayleigh waves dominated the zone near the surface, independent of the penetration depth. Furthermore, it was observed that the frequency content of ground vibrations reduces and peak values occur at lower frequency as the distance from the pile is increased.

Deeks(1992) presented a detailed study of dynamic soil-pile interaction in a simple (ideal) soil to develop a model based on fundamental soil parameters. He study a methodical manner through hammer impact, stress wave propagation in the pile, elastic shear wave radiation from the shaft, elastic wave radiation from the toe, the effect of soil inelasticity on the wave radiation, and finally the analysis of the complete pile-soil system. He developed a simplified model which represents the behavior of the ideal system extremely well, laying the basis for simplified models that may be calibrated in future work for field application.

He concluding that: a detailed study of pile driving dynamics has led to an improved model of pile-soil interaction which represents the theoretical behavior of a pile in an ideal soil extremely well. More complex finite element models can only achieve greater accuracy than the improved model when great care is exercised. The new model is a promising alternative to empirical models

in current use, and, once calibrated with field data, should find widespread application

### **2.3 Finite Element Method (FEM):**

Finite element method has been in recent years, widely used as a powerful tool in the analysis of engineering problems. In the numerical analysis, the behavior of the actual material is approximated with that of an idealized material that deforms in accordance with some constitutive relationships. Therefore, the choice of an appropriate constitutive model that adequately describes the behavior of the material plays an important role in the accuracy and reliability of the numerical predictions.

During the past few decades, several constitutive models have been developed for various materials, despite considerable complexities of constitutive theories, due to complex nature of some materials such as soils, rocks, composites etc. none of the existing constitutive models can completely describe the real behavior of these materials under various stress paths and loading conditions. At the beginning, the method is developed as an extension of a matrix method for the analysis of structural engineering problems. However, later it has also been recognized as the most powerful method for analyzing problems in other fields of engineering, such as fluid mechanics, soil mechanics, rock mechanics, heat flow, etc. The generation of its application coupled with the availability of high-speed electronic digital computer has put the finite element method in a wide range of use. In the finite element method, a continuum is divided into a number of elements. Each element consists of a number of nodes, and each node has a number of degrees of freedom that correspond to discrete values of the unknowns in the boundary value problem to

be solved, calculation with conventional methods can be useable if the problem has linear elastic behavior, most of the problems do not have linear elastic behavior, a numerical analysis program is reasonable when the problem cannot be solved by conventional methods based on analytic solutions. The basic idea in the finite element method is to divide a complicated model into a finite number of elements for which stresses and strains can be solved numerically.

Without going deep into the world of FEM, it can be mentioned that FEM is a technique to find approximate numerical solutions for partial differential equations as well for integral equations. This can be done by eliminating differential equations completely or rendering it to ordinary differential equations which can then be solved by other techniques (Euler's method etc.).

The basic concept of the FEM is that a complicated model of a body or structure is divided into a number of smaller elements. Those elements are then connected by nodes. At every node, there are one or more degrees of freedom where the number of functions is described. By solving the values at the nodes, the stress and strains in every element can be calculated. zienkiewicz and Taylor, 2005

## **2.4 General Information of PLAXIS 2D:**

PLAXIS 2D is two-dimensional finite element program developed for the analysis of deformation stability and ground water flow in geotechnical engineering it is a part of PLAXIS product range ,suite of finite element programs that is used worldwide for geotechnical engineering and design based on the finite element method. The program was originally developed at the University of Delft in Netherlands, the program is practical for solving complex



geotechnical problems involving settlement or slope stability, and real situation may be modeled either by plane strain or an axisymmetric model.

The program uses convenient graphical user interface that enable users to quickly generate a geometry model and finite element mesh based on a representative a vertical cross-section of the situation at hand.

The dynamic calculation program was developed in cooperation with the University of Joseph Fourier in Grenoble this cooperation is gratefully acknowledged .With the PLAXIS2D Dynamic analysis Module can be analyze the effects of vibrations in the soil.

In modeling the dynamic response of soil structure, the inertia of the sub soil and the Time dependence of the load are considered. Also, damping due to material and/or Geometry is taken in to account. Initially the Linear-elastic model can be utilized for the Simulation of the dynamic effects, but in principle any of the available soil models in PLAXIS can be used.

#### **2.4.1 Elements:**

The soil layers can be modeled by selecting either 6-node or 15-node triangular elements, as illustrated in Figure: 2.1. The 15 - node triangle has a fourth order interpolation for displacements and twelve stress points. The 6-node triangle has a second order interpolation for displacements and three stress points. The 15-node triangle is more useful for complicated problems but demands more memory consumption and results in a slightly slower calculation and operation performance. The 6-node triangle gives good result in standard deformation analyses but is not recommended in problems where failure plays

an important role. In those cases, the 15-node elements are recommended, (Brinkgreve 2006).

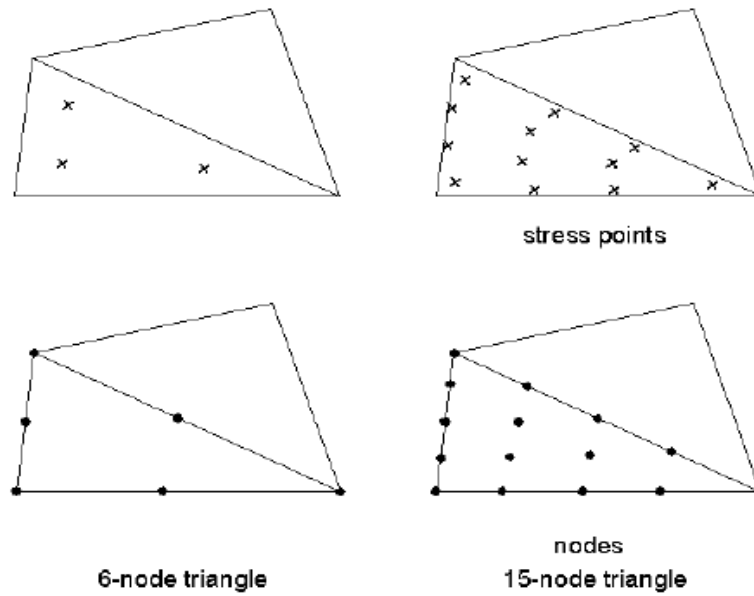


Figure 2.1 Nodes and stress point in -elements.(Brinkgreve 2006)

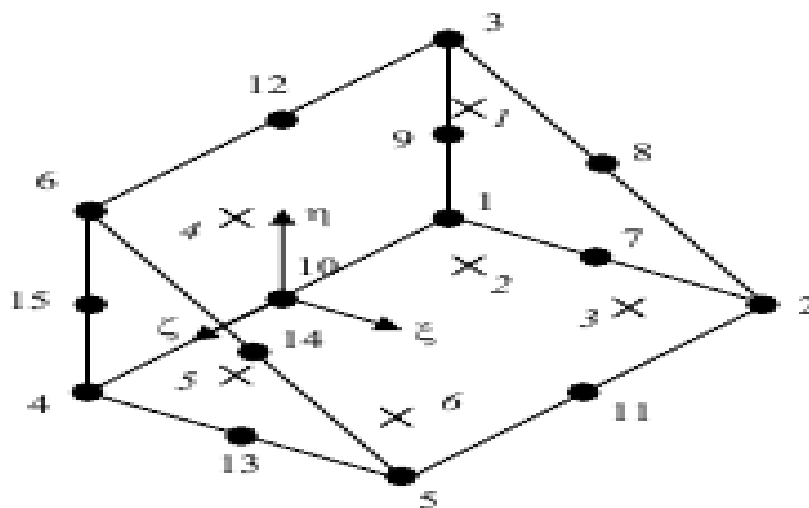
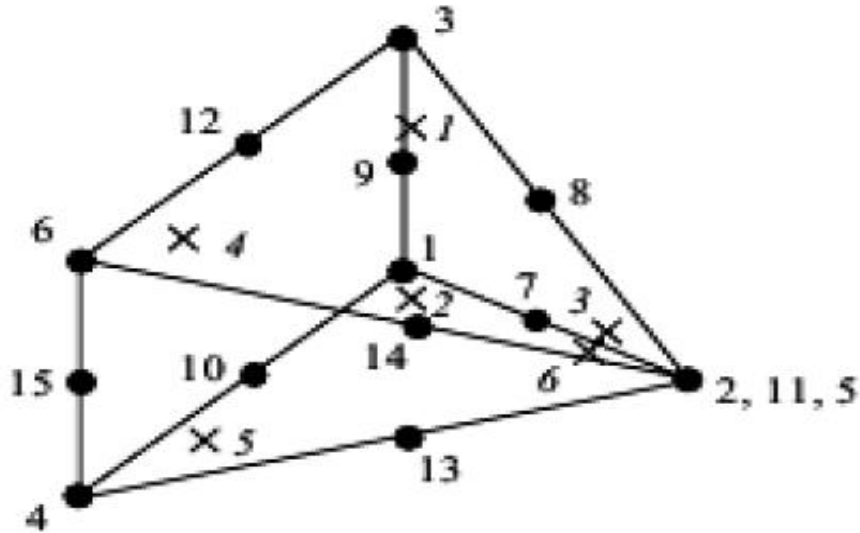


Figure 2.2 Distribution of nodes and stress points



**Figure 2.3 local numbering and positioning of nodes ( $\Sigma$ ) and integration points (x) of one fold degenerated (reduced) 15-node wedge element**

#### **2.4.2 Interface element:**

The interface elements allow relative displacement in terms of slipping and gapping. Interfaces can be used to simulate intensely shearing zone in contact with the pile, with values of friction angle and adhesion different to the friction angle and cohesion of the soil

Each interface has assigned to it a 'virtual thickness' which is an imaginary dimension used to define the material properties of the interface. The higher the virtual thickness is, the more elastic deformations are generated. In general, interface elements are supposed to generate very little elastic deformations and therefore the virtual thickness should be small. On the other hand, if the virtual thickness is too small, numerical ill-conditioning may occur. The virtual thickness is calculated as the Virtual thickness factor times the average element size. Interface elements are generally modeled by means of the bilinear Mohr-Coulomb model. When a more advanced model is used for the corresponding

cluster material data set, the interface element will only pick up the relevant data ( $\mathbf{C}, \psi, \mathbf{E}, \nu$ ) for the Mohr Coulomb model, In such cases the interface stiffness is taken to be the elastic soil stiffness. Hence,  $E = E_{ur}$  where  $E_{ur}$  is Stress level dependent, following a power law with  $E_{ur}$  proportional to  $\sigma^m$  (stress to the Power  $m$ ). For the Soft-Soil model, the Soft Soil Creep model and the Modified Cam Clay model, the power  $m$  is equal to 1 and  $E_{ur}$  is largely determined by the swelling constant  $\mathbf{K}^*$ .

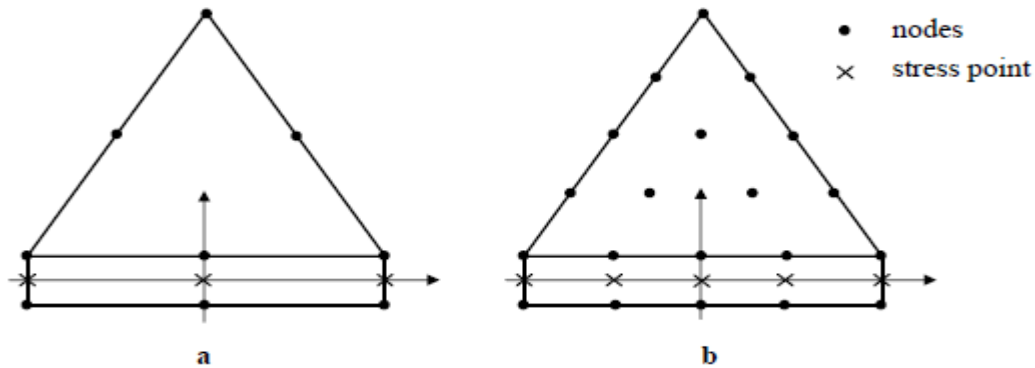


**Figure: 2.4 distribution of points, nodes and stress in the interface element and their connection to soil element**

### 2.4.3 Analysis types:

There are many types of analysis to be chosen from PLAXIS; Plastic analysis, dynamic analysis, Consolidation analysis and Phi-c reduction.

Plastic analysis can be selected when the user is interested in an elastoplastic deformation analysis in which it is not essential to take into account the magnitude of excess pore pressures with time. Plastic analysis does not take time effects into account. Plastic analysis can also be used with soft soils but the loading history and consolidation cannot be followed, instead, a reasonably accurate prediction of the final situation will be given.

The consolidation analysis should be used when it is of interest to follow the development of excess pore pressure with time in soft soils.

The phi-c reduction is a safety analysis in PLAXIS which is desired to use when the situation in the problem needs a calculation of the safety factor.

A safety analysis can be made after each individual calculation phase but it is recommended to use a safety analysis at the end when all calculation phases have been defined. Especially it is not advisable to start the calculation with a safety analysis as a starting condition for another calculation phase because this will end up in a state of failure (Brinkgreve 2006).

A dynamic calculation can be defined by selecting Dynamic analysis in the Calculation Type box of the General tab sheet. With PLAXIS it is possible to perform a dynamic analysis after series of plastic calculations.

#### **2.4.4 Material models:**

There are different material models to choose between in PLAXIS. The difference between those models is in how accurate they present the mechanical behavior of soils. The design of each model is to describe the relation between stress and strain in the material.

A short presentation of each model will be given before explaining in more detail those models that have been used.

- **Linear Elastic model (LE)**

The linear, isotropic elasticity is the simplest stress-strain relation that is available in PLAXIS. This model has only two input parameters, Young's modulus,  $E$ , and Poisson's ratio,  $\nu$ . Such a model is not appreciable to explain the complex behavior of soil but it is suitable for modeling massive structural elements and bedrock layers.

- **Mohr-Coulomb model (MC)**

Mohr-Coulomb is an elastic-plastic model involving five input parameters,  $E$  and  $\nu$  for soil elasticity,  $\phi$  and  $c$  for soil plasticity and  $\psi$  as an angle of dilatancy. To get a first assessment of deformations, it is according to Brinkgreve (2006) advisable to use the Mohr-Coulomb. This because other advanced models need further soil data than Mohr-Coulomb.

- **Jointed Rock model (JR)**

The Jointed Rock model is an anisotropic elastic-plastic model which is especially compliant for generating layers of rock involving stratified and specific fault directions. Plasticity can occur in a maximum of three shear planes where each plane has its own strength parameters,  $\phi$  and  $c$ . If the material has constant stiffness properties such as  $E$  and  $\nu$  then the intact rock will behave fully elastic while reduced elastic properties may be defined for the stratification direction.

- **Hardening-Soil model (HS)**

The Hardening Soil model is similar to the Mohr-Coulomb model but it is more advanced. As for Mohr-Coulomb, the input parameters of the Hardening Soil model are the friction angle, the cohesion and the dilatancy angle. The difference from Mohr-Coulomb model is that Hardening Soil model uses a three different input stiffness's: the triaxial loading stiffness,  $E_{50}$ , the triaxial unloading stiffness,  $E_{ur}$ , and the odometer loading stiffness,  $E_{oed}$ . For many soil types, it can be assumed that  $E_{ur} \approx 3E_{50}$  and  $E_{oed}$  another difference from the Mohr-Coulomb model is that stiffness's in the Hardening Soil model increase with pressure. The Hardening-Soil model is suitable for all soils but does not account for viscous effects such as creep and stress relaxation (generally all soils exhibit some creep).

- **Soft Soil model (SS)**

Soft Soil model is a Cam Clay type model that is used for computing primary compression of near normally-consolidated clay-type soils. According to Brinkgreve (2006), the Hardening Soil model outshines the Soft Soil model but it is still retained because older users of PLAXIS might be comfortable with this model.

- **Soft Soil Creep model (SSC):**

The secondary compression mostly happens in soft soil such as normally consolidated clays, silts and peat why this model has been specially developed for this purpose. Brinkgreve (2006) mentions that Soft Soil Creep model is not much better than the Mohr-Coulomb model in unloading problems such as tunneling and excavation.  $\approx E_{50}$  although very soft and very stiff soils can give other ratios.

- **Modified Cam Clay model (MCC)**

This model is well known from the international modeling literature. It has been added to PLAXIS recently to compete with other codes. Primary the aim with this model is to enable modeling of near normally consolidated clay soils.

## **2.5 Pile foundation:**

Piles are structural members that are made of steel, concrete or timber. They are used to build pile foundations, which are deep and which cost more than shallow foundations. Despite the cost, the use of piles often is necessary to ensure structural safety.

Piles may be divided into two categories based on the nature of their displacement: Displacement piles and non-displacement piles.

Driven piles are displacement pile because they move some soil laterally; hence, there is a tendency for densification of soil surrounding them.

Concrete piles and closed-ended pipe piles are high-displacement piles. However, steel H-piles displace less soil laterally during driving, so they are low displacement piles.

Piles are commonly used Fig: 2.5 for the following purposes:

- To carry the superstructure loads into or through a soil stratum. Both vertical and lateral loads may be involved.
- To resist uplift, or overturning, forces, such as for basement mats below the water table or to support tower legs subjected to overturning from lateral loads such as wind.
- To compact loose, cohesion less deposits through a combination of pile volume displacement and driving vibrations. These piles may be later pulled.
- To control settlements when spread footings or a mat is on a marginal soil or is underlain by a highly compressible stratum.
- To stiffen the soil beneath machine foundations to control both amplitudes of vibration and the natural frequency of the system.
- As an additional safety factor beneath bridge abutments and/or piers, particularly if scour is a potential problem.
- In offshore construction to transmit loads above the water surface through the water and into the underlying soil. Piles are sometimes used to control earth movements (for example, landslides).



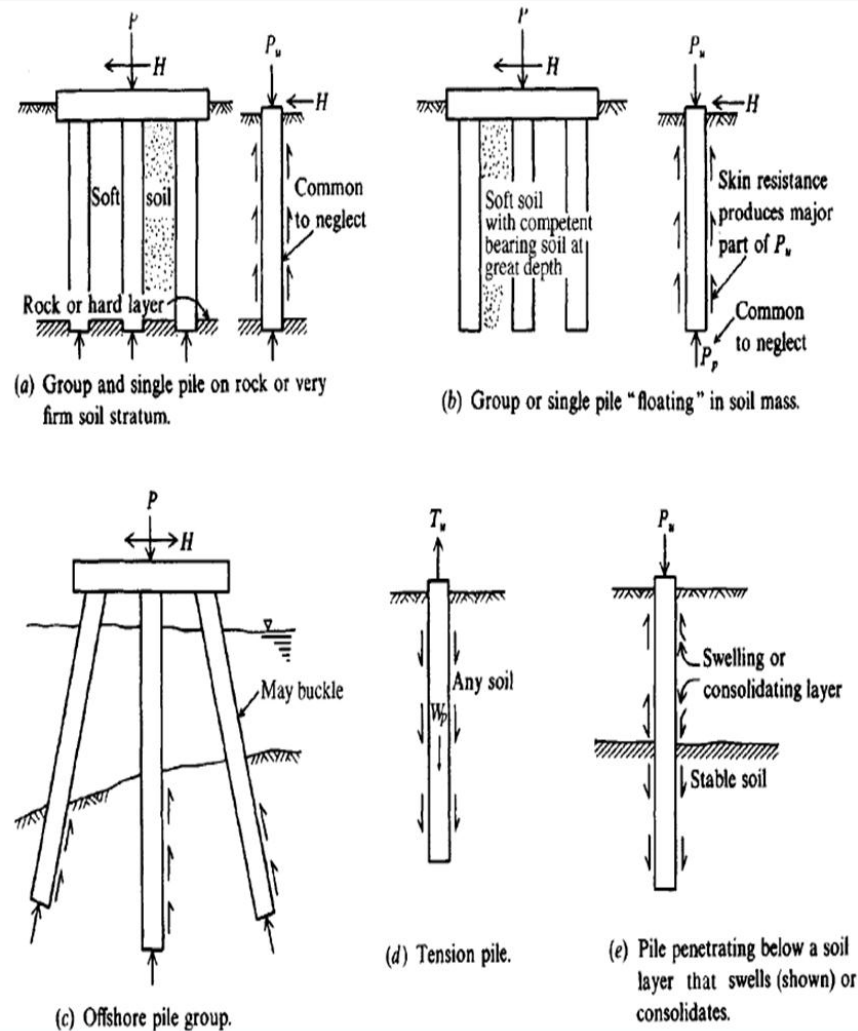


Figure: 2.5 pile configurations. (Bowles 1997)

### 2.5.1 The methods of inserted Piles into the soil:

- Driving with a steady succession of blows on the top of the pile using a pile hammer. This produces both considerable noise and local vibrations, hammers may be: Drop Hammers, Single, Acting Hammers, diesel Hammers
- Driving using a vibratory device attached to the top of the pile. This method is usually relatively quiet, and driving vibrations may not be excessive. The method is more applicable in deposits with little cohesion. The advantages of

the vibratory driver are: Reduced driving vibrations, reduced noise, and Great speed of penetration

- Drilling a hole and either inserting a pile into it or, more commonly, filling the cavity with concrete, which produces a pile upon hardening. A number of methods exist for this technique, Fig: 2.6
- Piles may also be inserted by jetting or partial auguring that is a high pressure stream of water is applied at the pile point to displace the soil.
- Jacking the pile is more applicable technique for short stiff members.

## **2.6 Some phenomena in expansive caused by driving process:**

There is some phenomena related with the driving pile in expansive soil like heave or settlement The phenomena may be serious or not, depending on how were takes place, and may be more serious for point-bearing piles if they are driven to refusal and then heave takes place and since excessive settlements take place [Nordlund 1963].

The simplest method of restraining piles against uplift is to employ a pile shaft that is sufficiently long to take the whole of the uplift load in skin friction. In such cases the shaft resistance must be augmented by adding dead weight to the pile to overcome the uplift load, Adding dead weight to counteract uplift loading is not usually feasible or economical.

St John calculated that the first pull on a previously unloaded pile in clay would give an uplift resistance equal to the ultimate resistance in skin friction. However under conditions of cyclic loading, or creep caused by sustained loading, the uplift skin friction could fall from the peak to the residual value, particularly in the case of long piles. In the latter case it was stated that irreversible uplift movements will not occur until the peak cyclic shear stress is 80% of the ultimate static capacity. For short piles under sustained uplift

loading, consideration of creep may reduce the uplift resistance to 50% of the resistance in static compression

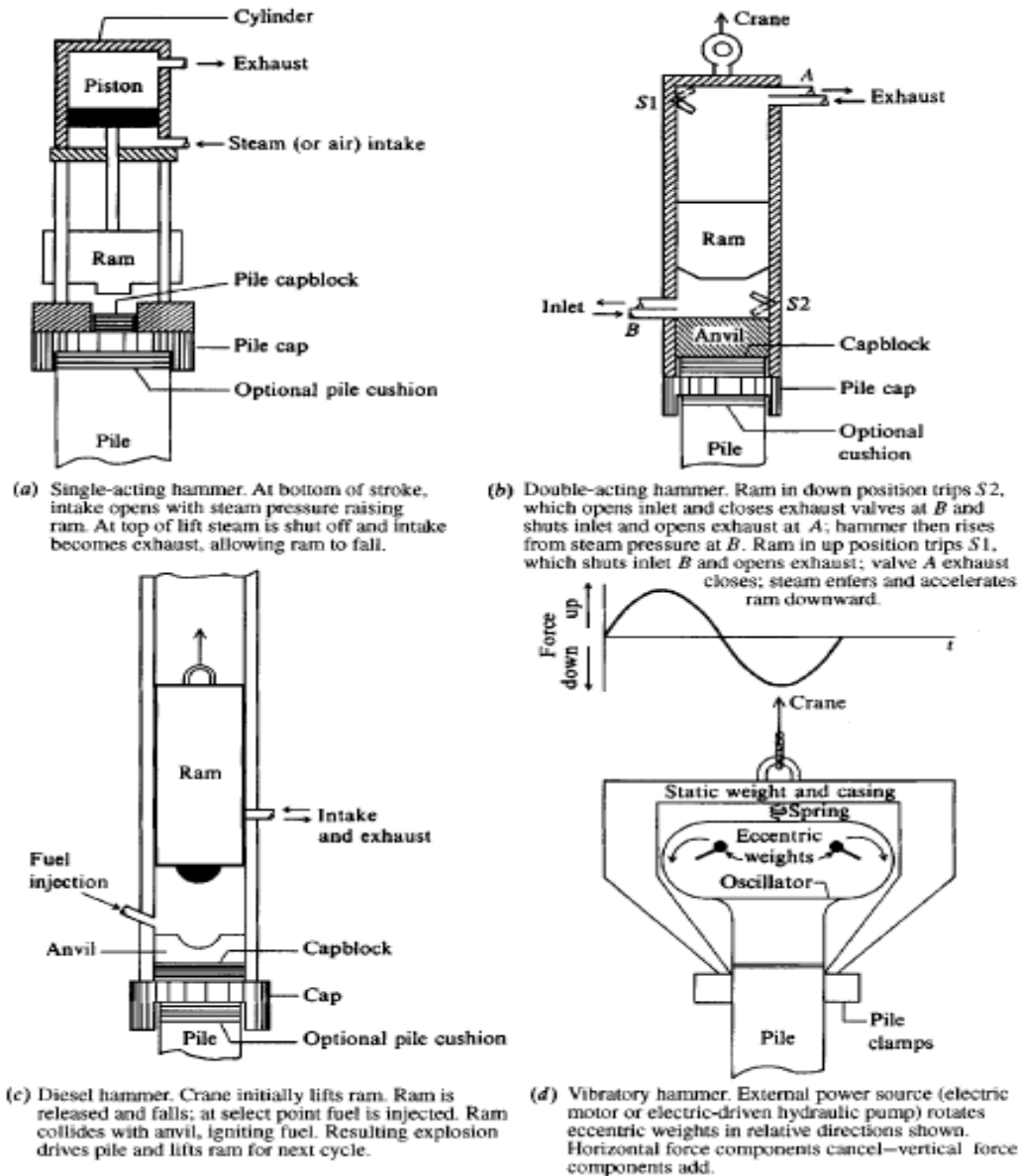


Figure 2.6 Schematics of several pile hammers.

### 2.6.1 Pile Heave:

Pile heave is a phenomenon where displacement of soil from pile penetration causes vertical or horizontal movement in nearby, previously driven piles.

Pile heave generally occurs in insensitive clays that behave as incompressible materials during pile driving, pile heave is important because redriving piles can require significant additional time and effort. The problem may or may not be serious, depending on how the heave takes place [Nordlund 1963].

### **2.6.2 Procedure to control Heave:**

- Heave can be controlled by predrilling an undersized hole for timber and closed-end pipe piles to reduce the volume displacement. Since heave is caused by volume displacement, it can be somewhat controlled by using small-volume displacement piles (HP or open-end pipes).
- If heave is anticipated, survey benchmarks should be established, and elevations taken on the piles after they are driven and as other piles are driven in the vicinity.
- Heave can be controlled by Pile driving may induce heave in saturated, fine-grained, non-quick-draining soils, where the displaced soil increases the pore water pressure so that the void ratio cannot rapidly change. As the pore pressure dissipates, the amount of heave may be reduced. Piles already driven in this material may be uplifted, the problem being especially aggravated if the piles are closely spaced.

### **2.6.3 Settlements:**

When piles are driven into soft clay, a certain surrounding the clay becomes remolded or compressed and this induced the settlement.

The effect of soil movement and percussion during driving on the stability of any adjacent building, structure, land, street and services should be carefully

assessed, the amount of settlement or movement that they could tolerate, may be obtained from the relevant government departments and utility companies.

The usual range of acceptable maximum total settlement for frame building in Korea follows recommendation by the Korean Society of Architectural Engineers (2004) and ranges from 100 mm to 150 mm for total settlement and 20 mm to 60 mm for differential settlement. Holt (1994) suggests a total settlement rang of 50 mm to 100 mm and differential settlement of 1:500 for frame buildings. The settlement on the ground is the sum of four parts:

#### **2.6.4 Immediate Settlement:**

This is commonly referred to as initial or undrained settlement and take place on account of shear strains which occur instantaneously following the application of the load. If the clay is saturated, settlements take place at constant volume caused by shear strains beneath the loaded area.

#### **2.6.5 Consolidation Settlement:**

Consolidation settlement or (primary consolidation settlement) happens when an increase in the effective vertical stress, occurs which gives rise to a decrease in the volume of the voids. If the soil is saturated ( $S_r=100\%$ ) reduction in volume occurs only if some of the pore water is squeezed out of the soil.

#### **2.6.6 Secondary Compression Settlement:**

Secondary compression is supposed to start after the primary consolidation ceases which is after the excess pore water pressure approaches zero, but it has not to be zero. Secondary compression takes place mostly in highly plastic

clays, organic soils and sanitary landfills. Secondary compression does not depend on changes in vertical effective stress.

#### **2.6.7 Distortion Settlement:**

Distortion settlement is a kind of settlement that develops from lateral movements of the soil because of changes in vertical effective stress. This happens when a heavy load is applied

#### **2.6.8 Procedure to control settlement:**

The settlement can be reduced with the following procedure before the driving process:

- The type of piles is very important. Low soil displacement piles reduce the volume of soil displaced during pile driving.
- Predrilled holes improve conditions for using displacement piles. The cross section of the auger and the drilled depth can strongly affect the volume of soil movements.
- The spacing of the piles characterized by the average pile density per unit foundation area affects soil movements: the bigger the density the larger the movement.
- The sequence of pile driving operations should be directed away from the existing structures.

# CHAPTER THREE

## THEORETICAL BACKGROUND

### 3.1 Introduction:

This chapter highlights the finite elements theory and basic equation of a dynamic modeling and a dynamic calculation describes in PLAXIS2D program

### 3.2 Basic Equation of Dynamic Behavior:

The basic equation for the time-dependent movement of a volume under the influence of a dynamic load is:

$$M\ddot{u} + C\dot{u} + Ku = F \quad 3.1$$

Here,  $M$  is the mass matrix,  $u$  is the displacement vector,  $C$  is the damping matrix,  $K$  is the stiffness matrix and  $F$  is the load vector. The displacement,  $u$ , the velocity,  $\dot{u}$ , and the Acceleration,  $\ddot{u}$ , can vary with time. The last two terms in the Eq 3.1 ( $Ku=F$ ) Correspond to the static deformation.

Here the theory is described on the bases of linear elasticity. However, in principle, all models in PLAXIS can be used for dynamic analysis. The soil behavior can be both drained and undrained. In the latter case, the bulk stiffness of the ground water is added to the stiffness matrix  $K$  is the case for the static calculation.

In the matrix  $M$  the mass of the materials (soil+water+ any constructions) is taken into account. In PLAXIS the mass matrix is implemented as a lumped matrix. The matrix  $C$  represents the material damping of the materials.

In reality, material damping is caused by friction or by irreversible deformations (plasticity or viscosity). With more viscosity more plasticity, more vibration energy can be dissipated. If elasticity is assumed, damping can still be taken in to account using the matrix  $C$ . To determine the damping matrix, extra parameters are required, which are difficult to determine from tests.

In finite element formulations,  $C$  is often formulated as a function of the mass and Stiffness matrices (Rayleigh damping) (Zienkiewicz&Taylor 1991) as:

$$C = \alpha_R M + \beta_R K \quad (2.3)$$

This limits the determination of the damping matrix to the Rayleigh coefficients  $\alpha_R$  and  $\beta_R$ . Here, when the contribution of  $M$  is dominant, for example,  $\alpha_R = 10^{-2}$  and  $\beta_R = 10^{-3}$  more of the low frequency vibrations are damped, and when the contribution of  $K$  is dominant for example,

$\alpha_R = 10^{-3}$  and  $\beta_R = 10^{-2}$  More of the high-frequency Vibrations are damped. In the standard setting of PLAXIS,  $\alpha_R = \beta_R = 0$

### 3.3 Time Integration:

In the numerical implementation of dynamics, the formulation of the time integration constitutes an important factor for the stability and accuracy of the calculation process. Explicit and implicit integration are the two commonly used time integration schemes.

The advantage of explicit integration is that it is relatively simple to formulate. However, the disadvantage is that the calculation process is not as robust and it imposes serious Limitations on the time step. The implicit method is more



complicated, but it produces more reliable (more stable) calculation process and usually a more accurate solution.

The implicit time integrations scheme of New mark is a frequently used method. With this method, the displacement and the velocity at the point in time  $t + \Delta t$  are expressed respectively as:

$$u^{t+\Delta t} = u^t + \dot{u}^t \Delta t + \left( \left( \frac{1}{2} - \alpha \right) \ddot{u}^t + \alpha \ddot{u}^{t+\Delta t} \right) \Delta t^2 \quad 3.3a$$

$$\dot{u}^{t+\Delta t} = \dot{u}^t + \left( (1 - \beta) \ddot{u}^t + \beta \ddot{u}^{t+\Delta t} \right) \Delta t \quad 3.3b$$

In the above equations,  $\Delta t$  is time step. The coefficients  $\alpha$  and  $\beta$  determine the accuracy of the numerical time integration, they are not equal to the  $\alpha$  and  $\beta$  for the Rayleigh damping. In order to obtain a stable solution, the following condition must apply:

$$\beta \geq 0.5 \quad \alpha \geq \frac{1}{4} \left( \frac{1}{2} + \beta \right)^2 \quad 3.4$$

The user is advised to use the standard setting of PLAXIS, in which the New mark Scheme with  $\alpha=0.25$  and  $\beta=0.50$  (average acceleration method) is utilized. Other Combinations are also possible, however. Implementation of the integrations scheme in PLAXIS Eq 3.3 can also be written as:

$$\begin{aligned} \ddot{u}^{t+\Delta t} &= c_0 \Delta u - c_2 \dot{u}^t - c_3 \ddot{u}^t \\ \dot{u}^{t+\Delta t} &= \dot{u}^t + c_6 \ddot{u}^t + c_7 \ddot{u}^{t+\Delta t} \\ u^{t+\Delta t} &= u^t + \Delta u \end{aligned} \quad 3.5a$$

Or as

$$\begin{aligned}\ddot{u}^{t+\Delta t} &= c_0 \Delta u - c_2 \dot{u}^t - c_3 \ddot{u}^t \\ \dot{u}^{t+\Delta t} &= c_1 \Delta u - c_4 \dot{u}^t - c_5 \ddot{u}^t \\ u^{t+\Delta t} &= u^t + \Delta u\end{aligned}\tag{3.5b}$$

where the coefficients  $c_0 \dots c_7$  can be expressed in the time step and in the integration parameters  $\alpha$  and  $\beta$ . In this way, the displacement, the velocity and the acceleration at the end of the time step are expressed by those at the start of the time step and the displacement increment, with implicit time integration Eq 3.1 must be obtained at the end of a time step ( $t + \Delta t$ )

$$M\ddot{u}^{t+\Delta t} + C\dot{u}^{t+\Delta t} + Ku^{t+\Delta t} = F\tag{3.6}$$

This equation, combined with the expressions (5.5) for the displacements, velocities and accelerations at the end of the time step, produce:

$$(c_0 M + c_1 C + K)\Delta u = F_{ext}^{t+\Delta t} + M(c_2 \dot{u}^t + c_3 \ddot{u}^t) + C(c_4 \dot{u}^t + c_5 \ddot{u}^t) + F_{int}^t\tag{3.7}$$

In this form, the system of equations for a dynamic analysis reasonably matches that of Static analysis. The difference is that the 'stiffness matrix' contains extra terms for mass  $S$  and damping and that the right-hand term contains extra terms specifying the velocity and Acceleration at the start of the time step (time  $\Delta t$ ).

### 3.3.1 Critical Time Step:

Despite the advantages of the implicit integration, the time step used in the calculation is subject to some limitations. If the time step is too large, the solution will display substantial deviations and the calculated response will be unreliable. The critical time Step depends on the maximum frequency and the

coarseness (finess) of the finite Element mesh. In general, the following expression can be used for single element.

$$\Delta t_{critical} = \frac{I_e}{\alpha \sqrt{\frac{E(1-\nu)}{\rho(1+\nu)(1-2\nu)}} \sqrt{1 + \frac{B^4}{4S^2} - \frac{B^2}{2S} \left[ 1 + \frac{1-2\nu}{4} \frac{2S}{B^2} \right]}} \quad 3.8$$

In the above equation, the term  $B$  and  $S$  respectively denote the largest dimension of the Finite element and the surface area of the finite element.

The first root term represent  $S$  the Velocity of a (compression) wave, Eq.3.12 in the Material Models Manual. The factor depends on the element type.

For a 6-node element  $\alpha = 1/(6\sqrt{c_6})$  with  $C_6 \approx 5.1282 \cdot 10^{-2}$ , and for a 15-node element  $\alpha = 1/19\sqrt{c_{15}}$  with  $C_{15} \approx 4.9479 \cdot 10^{-3}$  (Zienkiewicz & Taylor, 1991).

The other determining factors are the Poisson's ratio,  $\nu$ , and the average length of an element,  $l_e$ , (see the Reference Manual For adscription of the average element length). In a finite element model, the critical Time step is equal to the minimum value of  $\Delta t$  according to Eq. (3.8) over all elements.

This time step is chosen to ensure that wave during a single step does not move a distance larger than the minimum dimension of an element.

### 3.3.2 Wave Velocity:

The comparison wave velocity  $V_P$  in confined one-dimensional soil is a function of stiffness,  $E_{oed}$ , and the mass  $\rho$  as:

$$V_P = \sqrt{\frac{E_{oed}}{\rho}} \quad \text{Where} \quad E_{oed} = \frac{(1-\nu)E}{(1+\nu)(1-2\nu)} \quad \text{and} \quad \rho = \frac{\gamma_{unsat}}{g} \quad 3.9$$

In which  $E$ = Young modules,  $\nu$ =poissons ratio,  $\gamma$  =total unit weight and

$g$  =gravity Acceleration ( $9.8\text{m/S}^2$ ), a similar expression can be found for the shear wave velocity  $V_s$

$$V_s = \sqrt{\frac{G}{\rho}} \quad \text{Where } G = \frac{E}{2(1+\nu)} \quad \text{and } \rho = \frac{\gamma_{unsat}}{g} \quad 3.10$$

### 3.4 Model Boundaries:

In the case of a static deformation analysis, prescribed boundary displacements are introduced at the boundaries of a finite element model. The boundaries can be completely free or fixities can be applied in one or two directions .Particularly the vertical Boundaries of mesh are often non-physical (synthetic) boundaries that have been chosen so that they do not actually influence the deformation behavior of the construction to be modeled. In other words: the boundaries are ' far away' .For dynamic calculations, the boundaries should in principle be much further away than those for static calculations, because, otherwise, stress waves will be reflected leading to distortions in the computed results. However, locating the boundaries faraway requires many extra Element sand therefore a lot of extra memory and calculating time.To counteract reflections, special measures are needed at the boundaries-in this Context, we speak of 'silent or viscous boundaries'. Various methods are used to create these boundaries, which include:

- Use of half-infinite elements (boundary elements).
- Adaptation of the material properties of elements at the boundary (Low stiffness, high viscosity).
- Use of viscous boundaries (dampers).

All of these methods have their advantages and disadvantages and are problem dependent. For the implementation of dynamic effects in PLAXIS the viscous boundaries are created with the last method (use of viscous boundaries). The way this method works is described below.

### 3.5 Viscous Boundaries:

In opting for viscous boundaries, a damper is used instead of applying fixities in a certain direction. The damper ensures that an increase in stress on the boundary is absorbed without rebounding. The boundary then starts to move.

The use of viscous boundaries in PLAXIS is based on the method described by (Lysmer & Kuhlmeyer, 1969). The normal and shear stress components absorbed by a damper in x-direction are:

$$\sigma_n = -C_1 \rho V_p \dot{u}_x \quad 3.11a$$

$$\tau = -C_2 \rho V_s \dot{u}_y \quad 3.11b$$

Here,  $\rho$  is the density of the materials.  $V_p$  and  $V_s$  are the pressure wave velocity and the shear wave velocity, respectively.  $V_p$  and  $V_s$  are determined using Eq.3.12 and Eq.3.13 in the Material Models Manual.  $C_1$  and  $C_2$  are relaxation coefficients that have been introduced in order to improve the effect of the absorption. When pressure waves only strike the boundary perpendicular, relaxation is redundant ( $C_1=C_2=1$ ).

In the presence of shear waves, the damping effect of the viscous boundaries is not sufficient without relaxation. The effect can be improved by adapting the second Coefficient in particular.

The experience gained until now shows that the use of  $C_1=1$  and  $C_2=0.25$  results in a reasonable absorption of waves at the boundary.

However, it is not possible to state that shear waves are fully absorbed so that in the presence of shear waves a limited boundary effect is noticeable. Additional research is therefore necessary on this point, but the method described will be sufficient for practical applications.

For an inclined boundary, an adjusted formulation based on Eq. (3.11) is used that takes the angle of the boundary into account.

### **3.6 Initial Stresses and Stress Increments:**

By removing the boundary fixities during the transition from a static analysis to a dynamic analysis, the boundary stresses also cease. This means that the boundary will start to move as a result of initial stresses. To prevent this, the original boundary stress will be converted to an initial (virtual) boundary velocity.

When calculating the stress, the initial boundary velocity must be subtracted from the real velocity:

$$\sigma_n = -c_1 \rho V_P \dot{u}_n + \sigma_n^0 = -c_1 \rho V_P (\dot{u}_n - \dot{u}_n^0) \quad 3.12$$

This initial velocity is calculated at the start of the dynamic analysis and is therefore based purely on the original boundary stress (preceding calculation or initial stress state). At present, situations can arise where a new load is applied at certain location on the Model and is continuously present from that moment onward. Such a load should result in an increase in the average boundary stress. If

it involves a viscous boundary, the Average incremental stress cannot be absorbed. Instead, the boundary will start to move.

### **3.7 Linear Elastic-Perfectly Plastic Model (Mohr-Coulomb Model):**

Plasticity is associated with the development of irreversible strains. In order to evaluate whether or not plasticity occurs in a calculation, a yield function,  $f$ , is introduced as a function of stress and strain. Plastic yielding is related with the condition  $f = 0$ . This condition can often be presented as a surface in principal stress space. A perfectly plastic model is a constitutive model with a fixed yield surface, i.e. a yield surface that is fully defined by model parameters and not affected by (plastic) straining. For stress states represented by points within the yield surface, the behavior is purely elastic and all strains are reversible.

#### **3.7.1 Linear Elastic Perfectly-Plastic Behavior:**

The basic principle of elastoplasticity is that strains and strain rates are decomposed into an elastic part and a plastic part as shown in figure 3.1:

$$\varepsilon = \varepsilon^e + \varepsilon^P \quad \dot{\varepsilon} = \dot{\varepsilon}_e + \dot{\varepsilon}_P \quad 3.13$$

Hooke's law is used to relate the stress rates to the elastic strain rates. Substitution of Eq. (2.5) into Hooke's law leads to:

$$\dot{\sigma} = D^e \dot{\varepsilon}^e = D^e (\dot{\varepsilon} - \dot{\varepsilon}^P) \quad 3.14$$

According to the classical theory of plasticity (Hill, 1950), plastic strain rates is proportional to the derivative of the yield function with respect to the stresses. This means that the plastic strain rates can be represented as vectors

perpendicular to the yield surface. This classical form of the theory is referred to as associated plasticity. However, for Mohr-Coulomb type yield functions, the theory of associated plasticity overestimates dilatancy.

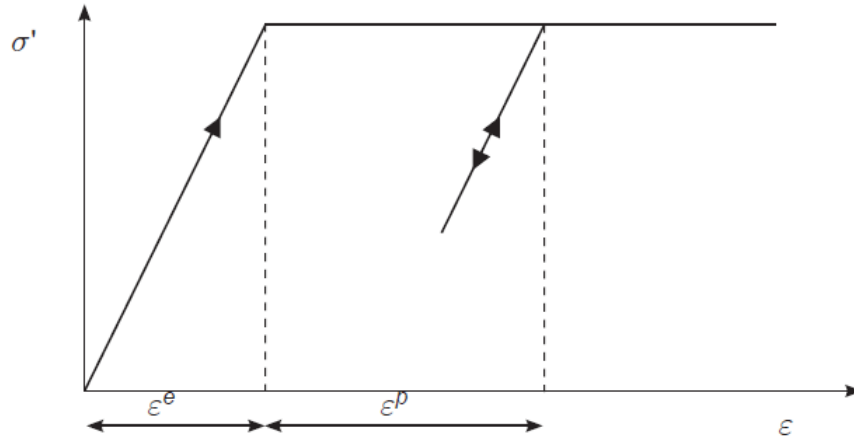


Figure: 3.1 Basic idea of an elastic perfectly plastic model

Therefore, in addition to the yield function, a plastic potential function  $g$  is introduced as non-associated plasticity. In general, the plastic strain rates are written as:

$$\dot{\varepsilon}^P = \lambda \frac{\partial g}{\partial \sigma} \quad 3.15$$

In which  $\lambda$  is the plastic multiplier. For purely elastic behavior  $\lambda$  is zero, whereas in the case of plastic behavior  $\lambda$  is positive:

$$\lambda = 0 \text{ for: } f < 0 \quad \text{or:} \quad \frac{\partial f^T}{\partial \sigma} D^e \dot{\varepsilon} \leq 0 \quad (\text{Elasticity}) \quad 3.16a$$

$$\lambda = 0 \text{ for: } f = 0 \quad \text{and:} \quad \frac{\partial f^T}{\partial \sigma} D^e \dot{\varepsilon} > 0 \quad (\text{Plasticity}) \quad 3.16$$



These equations may be used to obtain the following relationship between the effective stress rates and strain rates for elastic-perfectly-plastic behavior (Smith & Griffith, 1982; Vermeer & Borst, 1984):

$$\dot{\sigma} = \left( D^e - \frac{\alpha}{d} D^e \frac{\partial g}{\partial \sigma} \frac{\partial f^T}{\partial \sigma} D^e \right) \dot{\varepsilon} \quad 3.17a$$

$$d = \frac{\partial f^T}{\partial \sigma} D^e \frac{\partial g}{\partial \sigma} \quad 3.17b$$

The parameter  $\alpha$  is used as a switch. If the material behavior is elastic, as defined by Eq. (3.4a), the value of  $\alpha$  is equal to zero, whilst for plasticity, as defined by Eq. (3.4b), the value of  $\alpha$  is equal to unity. The above theory of plasticity is restricted to smooth yield surfaces and does not cover a multi-surface yield contour as present in the full Mohr-Coulomb model.

For such a yield surface, the theory of plasticity has been extended by Koiter (1960) and others to account for flow vertices involving two or more plastic potential functions:

$$\dot{\varepsilon}^p = \lambda_1 \frac{\partial g_1}{\partial \sigma} + \lambda_2 \frac{\partial g_2}{\partial \sigma} + \dots \quad 3.18$$

Similarly, several quasi-independent yield functions ( $f_1, f_2 \dots$ ) are used to determine the magnitude of the multipliers ( $\lambda_1, \lambda_2 \dots$ ).

### 3.7.2 Formulation of the Mohr-Coulomb Model:

The Mohr-Coulomb yield condition is an extension of Coulomb's friction law to general states of stress. In fact, this condition ensures that Coulomb's friction law is obeyed in any plane within a material element.

The full Mohr-Coulomb yield condition consists of six yield functions when formulated in terms of the two plastic model parameters appearing in the yield functions are the well-known friction angle  $\phi$  and the cohesion  $c$ . The condition  $f_i = 0$  for all yield functions together (where  $f_i$  is used to denote each individual yield function) represents a fixed hexagonal cone in principal stress space as shown in Figure 3.2. Principal stresses:

$$f_{1a} = \frac{1}{2} (\sigma_2 - \sigma_3) + \frac{1}{2} (\sigma_2 + \sigma_3) \sin \phi - c \cos \phi \leq 0 \quad 3.18a$$

$$f_{1b} = \frac{1}{2} (\sigma_3 - \sigma_2) + \frac{1}{2} (\sigma_3 + \sigma_2) \sin \phi - c \cos \phi \leq 0 \quad 3.18b$$

$$f_{2a} = \frac{1}{2} (\sigma_3 - \sigma_1) + \frac{1}{2} (\sigma_3 + \sigma_1) \sin \phi - c \cos \phi \leq 0 \quad 3.18c$$

$$f_{2b} = \frac{1}{2} (\sigma_1 - \sigma_3) + \frac{1}{2} (\sigma_1 + \sigma_3) \sin \phi - c \cos \phi \leq 0 \quad 3.18d$$

$$f_{3a} = \frac{1}{2} (\sigma_1 - \sigma_2) + \frac{1}{2} (\sigma_1 + \sigma_2) \sin \phi - c \cos \phi \leq 0 \quad 3.18e$$

$$f_{3b} = \frac{1}{2} (\sigma_2 - \sigma_1) + \frac{1}{2} (\sigma_2 + \sigma_1) \sin \phi - c \cos \phi \leq 0 \quad 3.18f$$

The two plastic model parameters appearing in the yield functions are the well-known friction angle  $\phi$  and the cohesion  $c$ . The condition  $f_i = 0$  for all yield functions together (where  $f_i$  is used to denote each individual yield function) represents a fixed hexagonal cone in principal stress space as shown in Figure 3.2.

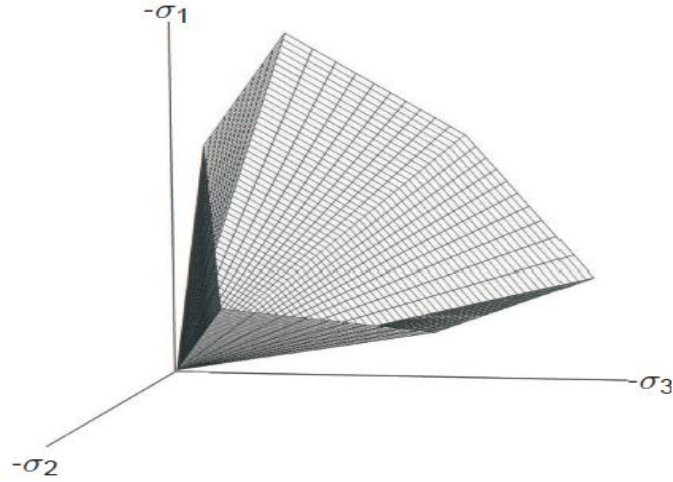


Figure 3.2 the Mohr coulomb yield surface in principle stress space (C=0)

In addition to the yield functions, six plastic potential functions are defined for the Mohr-Coulomb model:

$$g_{1a} = \frac{1}{2} (\sigma_2 - \sigma_3) + \frac{1}{2} (\sigma_2 + \sigma_3) \sin \psi \quad 3.19a$$

$$g_{1b} = \frac{1}{2} (\sigma_3 - \sigma_2) + \frac{1}{2} (\sigma_3 + \sigma_2) \sin \psi \quad 3.19b$$

$$g_{2a} = \frac{1}{2} (\sigma_3 - \sigma_1) + \frac{1}{2} (\sigma_3 + \sigma_1) \sin \psi \quad 3.19c$$

$$g_{2b} = \frac{1}{2} (\sigma_1 - \sigma_3) + \frac{1}{2} (\sigma_1 + \sigma_3) \sin \psi \quad 3.19d$$

$$g_{3a} = \frac{1}{2} (\sigma_1 - \sigma_2) + \frac{1}{2} (\sigma_1 + \sigma_2) \sin \psi \quad 3.19e$$

$$f_{3b} = \frac{1}{2} (\sigma_2 - \sigma_1) + \frac{1}{2} (\sigma_2 + \sigma_1) \sin \psi \quad 3.19f$$

The plastic potential functions contain a third plasticity parameter, the dilatancy angle  $\psi$ . This parameter is required to model positive plastic volumetric strain increments, dilatancy as actually observed for dense soils. A discussion of the entire model parameters used in the Mohr-Coulomb model is given in the next section.

When implementing the Mohr-Coulomb model for general stress states, special treatment is required for the intersection of two yield surfaces. Some programs use a smooth transition from one yield surface to another.

In PLAXIS, however, the exact form of the full Mohr-Coulomb model is implemented, using a sharp transition from one yield surface to another.

For  $c > 0$ , the standard Mohr-Coulomb criterion allows for tension. In fact, allowable tensile stresses increase with cohesion. In reality, soil can sustain none or only very small tensile stresses. This behavior can be included in a PLAXIS analysis by specifying a tension cut-off. In this case, Mohr circles with positive principal stresses are not allowed. The tension cut-off introduces three additional yield functions, defined as:

$$f_4 = \sigma_1 - \sigma_t \leq 0 \quad 3.20a$$

$$f_5 = \sigma_2 - \sigma_t \leq 0 \quad 3.20b$$

$$f_6 = \sigma_3 - \sigma_t \leq 0 \quad 3.20c$$

When this tension cut-off procedure is used, the allowable tensile stress,  $\sigma_t$  is by default, taken equal to zero, but this value can be changed by the user. For these three yield functions, an associated flow rule is adopted.

For stress states within the yield surface, the behavior is elastic and obeys Hooke's law for isotropic linear elasticity. Hence, besides the plasticity parameters  $c$ ,  $\phi$ , and  $\psi$ , the input is required on the elastic Young's modulus  $E$  and Poisson's ratio  $\nu$ . The model described here is officially called the linear elastic perfectly plastic model with Mohr-Coulomb failure criterion. For simplicity, this model is called the Mohr-Coulomb model in PLAXIS

### 3.7.3 Basic Parameters of the Mohr-Coulomb Model:

The linear elastic-perfectly-plastic Mohr-Coulomb model requires a total of five parameters, which are generally familiar to most geotechnical engineers and which can be obtained from Basic tests on soil samples as shown in Figure 3.4. These parameters with their standard units are listed below:

$E$ :	<i>Yong's modulus</i>	$[kn/m^2]$
$\nu$ :	<i>Poisson's ratio</i>	$[-]$
$c$ :	<i>Cohesion</i>	$[KN/m^2]$
$\varphi$ :	Friction angle	$[^\circ]$
$\psi$ :	Dilatancy angle	$[^\circ]$
$\sigma_t$ :	Tension cut-off and tensile strength	$[kN/m^2]$

Instead of using the Young's modulus as a stiffness parameter, alternative stiffness parameters can be entered. These parameters with their standard units are listed below:

$G$ :	Shear modulus $[kN/m^2]$
$E_{oed}$ :	Odometer modulus $[kN/m^2]$

Parameters can either be effective parameters (indicated by a dash sign '-') or undrained parameters (indicated by a subscript u), depending on the selected drainage type. In the case of dynamic applications, alternative and/or additional parameters may be used to define stiffness based on wave velocities. These parameters are listed below:

$V_p =$  Compression wave velocity [m/s]

$V_s =$  Shear wave velocity [m/s]

#### **3.7.4 Young's modulus (E):**

PLAXIS uses the Young's modulus as the basic stiffness modulus in the elastic model and the Mohr-Coulomb model, but some alternative stiffness module is displayed as well. A stiffness modulus has the dimension of stress. The values of the stiffness parameter adopted in a calculation require special attention as many geometrical show a non-linear behavior from the very beginning of loading. In triaxial testing of soil samples the initial slope of the stress-strain curve (tangent modulus) is usually indicated as  $E_0$  and the secant modulus at 50% strength is denoted as  $E_{50}$  see Figure 3.3. For materials with a large linear elastic range it is realistic to use  $E_0$ , but for loading of soils, one generally uses  $E_{50}$ . Considering unloading problems, as in the case of tunneling and excavations, one needs an unload-reload modulus ( $E_{ur}$ ) instead of  $E_{50}$ . For soils, both the unloading modulus,  $E_{ur}$ , and the first loading modulus,  $E_{50}$ , tend to increase with the confining pressure. Hence, deep soil layers tend to have a greater stiffness than shallow layers. Moreover, the observed stiffness depends on the stress path that is followed. The stiffness is much higher for unloading and reloading than for primary loading. Also, the observed soil stiffness in terms of a Young's modulus may be lower for (drained) compression than for shearing. Hence, when using a constant stiffness modulus to represent soil behavior one should choose a value that is consistent with the stress level and the stress path development.

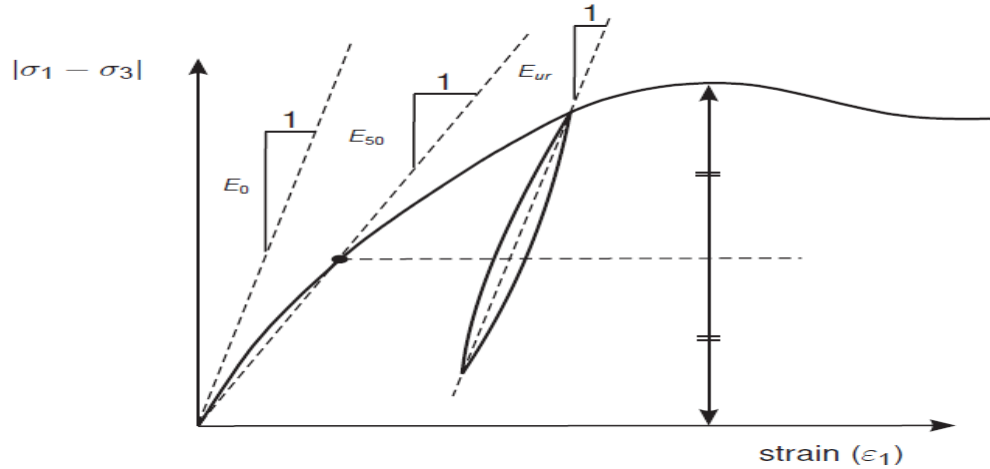


Figure: 3.3 Definition of  $E_0$  and  $E_{50}$  for standard drained triaxial test result

### 3.7.5 Poisson's ratio ( $\nu$ ):

Drained triaxial tests may yield a significant rate of volume decrease at the very beginning of axial loading and consequently, a low initial value of Poisson's ratio ( $\nu_0$ ). For some cases, such as particular unloading problems, it may be realistic to use such a low initial value, but in general, when using the Mohr-Coulomb model the use of a higher value is recommended.

The selection of a Poisson's ratio is particularly simple when the elastic model or Mohr-Coulomb model is used for gravity loading. For this type of loading, PLAXIS should give realistic ratios of  $K_0 = \sigma_h / \sigma_v$ .

As both models will give the well-known ratio of  $\sigma_h / \sigma_v = \nu / (1 - \nu)$  for one-dimensional compression it is easy to select a Poisson's ratio that gives a realistic value of  $K_0$ . Hence,  $\nu$  is evaluated by matching  $K_0$ .

### 3.7.6 Cohesion (c):

The cohesive strength has the dimension of stress. In the Mohr-Coulomb model, the cohesion parameter may be used to model the effective cohesion  $c'$  of the soil, in combination with a realistic effective friction angle  $\phi$ .

### 3.7.7 Friction angle ( $\phi$ ):

The friction angle  $\phi$  (phi) is entered in degrees. In general, the friction angle is used to model the effective friction of the soil, in combination with an effective cohesion  $c'$

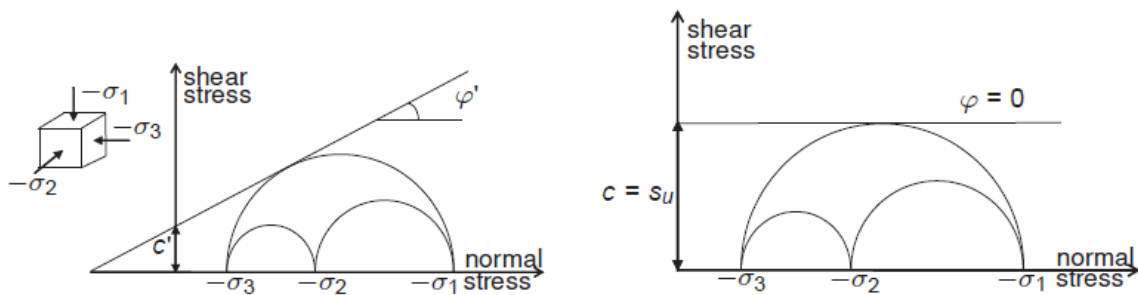


Figure: 3.4 stress circle at yield ;one touches coulomb envelope

### 3.7.8 Dilatancy angle ( $\psi$ ):

The dilatancy angle,  $\psi$  (psi), is specified in degrees. Apart from heavily over-consolidated layers, clay soil tends to show little dilatancy. The dilatancy of sand depends on both the density and on the friction angle. In general, the dilatancy angle of soils is much smaller than the friction angle.

### 3.7.9 Shear modulus (G):

The shear modulus,  $G$ , has the dimension of stress. According to Hooke's law, the relationship between Young's modulus  $E$  and the shear modulus is given by



$$G = \frac{E}{2(1+\nu)} \quad 3.21$$

Entering a particular value for one of the alternatives  $G$  or  $E_{\text{oed}}$  results in a change of the  $E$  modulus whilst  $\nu$  remains the same.

### 3.7.10 Odometer modulus ( $E_{\text{oed}}$ ):

The odometer modulus,  $E_{\text{oed}}$ , has the dimension of stress. According to Hooke's law, the relationship between Young's modulus  $E$  and the shear modulus is given by

$$E_{\text{oed}} = \frac{(1 - \nu)E}{(1 - 2\nu)(1 + \nu)} \quad 3.22$$

Entering a particular value for one of the alternatives  $G$  or  $E_{\text{oed}}$  results in a change of the  $E$  modulus whilst  $\nu$  remains the same.

## 3.8 Advanced Parameters of Mohr-Coulomb model:

When using the Mohr-Coulomb model, the <Advanced> button in the *Parameters* tab sheet may be clicked to enter some additional parameters for advanced modeling features. As a result, an additional window appears as shown in Figure 3.5. The advanced features comprise the increase of stiffness and cohesive strength with depth and the use of a tension cut-off. In fact, the latter option is used by default, but it may be deactivated here if desired.

### 3.8.1 Increase of stiffness (Increment):

In real soils, the stiffness depends significantly on the stress level, which means that the stiffness generally increases with depth. When using the Mohr-Coulomb model, the stiffness is a constant value. In order to account for the

increase in the stiffness with the depth the Increment-value may be used, which is the increase of the Young's modulus per unit of depth (expressed in the unit of stress per unit depth). At the level given by the  $y_{ref}$  parameter, the stiffness is equal to the reference Young's modulus,  $E_{ref}$ , as entered in the Parameters tab sheet. The actual value of Young's modulus in the stress points is obtained from the reference value and  $E_{increment}$ .

Note that during calculations a stiffness increasing with depth does not change as a function of the stress state.

### **3.8.2 Increase of cohesion (increment):**

PLAXIS offers an advanced option for the input of clay layers in which the cohesion increases with depth. In order to account for the increase of the cohesion with the depth the increment-value may be used, which is the increase of cohesion per unit of depth (expressed in the unit of stress per unit depth).

At the level given by the  $y_{ref}$  parameter, the cohesion is equal to the (reference) cohesion,  $C_{ref}$ , as entered in the Parameters tab sheet. The actual value of cohesion in the stress points is obtained from the reference value and increment.

### **3.8.3 Tension cut-off:**

In some practical problems an area with tensile stresses may develop. According to the Coulomb envelope shown in Figure 2.3, this is allowed when the shear stress (radius of Mohr circle) is sufficiently small. However, the soil surface near a trench in clay sometimes shows tensile cracks. This indicates that soil may also fail in tension instead of in shear. Such behavior can be included in PLAXIS analysis by selecting the tension cut-off. In this case, Mohr circles with positive principal stresses are not allowed. When selecting the tension cut-

off, the allowable tensile strength may be entered. For the Mohr-Coulomb model and the Hardening-Soil model the tension, cut-off is, by default, selected with a tensile strength of zero.

### **3.9 Drainage Type:**

In principle, all model parameters in PLAXIS are meant to represent the effective soil response, i.e. the relationship between the stresses and the strains associated with the soil skeleton. An important feature of soil is the presence of pore water. Pore pressures significantly influence the (time-dependent) soil response. PLAXIS offers several options to enable incorporation of the water-skeleton interaction in the soil response. The most advanced option is a fully coupled flow-deformation analysis. However, in many cases, it is sufficient to analyze either the long-term (drained) response or the short-term (undrained) response without considering the time-dependent development of pore pressures. In the latter case (undrained), excess pore pressures are generated as a result of stress changes (loading or unloading). The dissipation of these excess pore pressures with time can be analyzed in a consolidation calculation. The simplified water-skeleton interaction, as considered in a Plastic calculation, a Safety analysis or a Dynamic analysis, is defined by the Drainage type parameter. PLAXIS offers a choice of different types of drainage:

#### **3.9.1 Drained Behavior:**

Using this setting no excess pore pressures are generated. This is clearly the case for dry soils and also for full drainage due to a high permeability (sands) and/or a low rate of loading..This option may also be used to simulate long-term soil behavior without the need to model the precise history of undrained loading and consolidation.

### **3.9.2 Undrained behavior:**

This setting is used for saturated soils in cases where pore water cannot freely flow through the soil skeleton. The flow of pore water can sometimes be neglected due to a low permeability (clays) and/or a high rate of loading. All clusters that are specified as undrained will indeed behave undrained, even if the cluster or a part of the cluster is located above the phreatic level.

### **3.9.3 Non-Porous Behavior:**

Using this setting neither initial nor excess pore pressures will be taken into account in clusters of this type. Applications may be found in the modeling of concrete or structural behavior. Non-porous behavior is often used in combination with the linear elastic model. The input of a saturated weight is not relevant for non-porous materials or intact rock.

## **3.10 Dynamic Model Parameters:**

Dynamic analysis does not, in principle, require additional model parameters. However, alternative and/or additional parameters may be used to define wave velocities and to include material damping.

Wave velocities  $V_p$  and  $V_s$  The material parameters are defined in the Parameters tab sheet of the Material Properties window.

When entering the elastic parameters  $E$  and  $\nu$ , the corresponding wave velocities  $V_p$  and  $V_s$  are automatically generated, provided that a proper unit weight has been specified. However, for Mohr-Coulomb and linear elastic models it can be entered the wave velocities  $V_p$  and  $V_s$  as an alternative for the

parameters  $E$  and  $\nu$ . The corresponding values for  $E$  and  $\nu$  will then be generated by PLAXIS,

Figure 3.5 Elastic parameters in Mohr-Coulomb and linear elastic models

### 3.10.1 Rayleigh alpha and beta:

Material damping in soils generally caused by its viscous properties, friction and the Development of plasticity; However, in PLAXIS the soil models do not include viscosity as such. Instead, a damping term is assumed, which is proportional to the mass and Stiffness of the system (Rayleigh damping), such that:

$$\mathbf{C} = \alpha \mathbf{M} + \beta \mathbf{K} \quad 3.23$$

Where C represents the damping, M the mass, K the stiffness and  $\alpha$  (alpha) and  $\beta$  (beta) are the Rayleigh coefficients. The standard settings in PLAXIS assume no Rayleigh damping (Rayleigh alpha and Rayleigh beta equal to 0.0). However, damping can be introduced in The Material data sets for soils and interfaces.

In single-source type of problems using an axisymmetric model, it may not be necessary to include Rayleigh damping, since most of the damping is caused by the radial Spreading of the waves (geometric damping).

### **3.10.2 Determination of the Rayleigh damping coefficients:**

It is well known fact that damping in soil structure influences significantly the magnitude and shape of its response .However and despite the considerable amount of research work in this field, little have yet been achieved for the development of a commonly accepted procedure for damping parameter identification .Instead, for Engineering purposes, some measures are made to account for the material and geometrical damping. Commonly used engineering parameter is the damping ratio.

In finite element method, the Rayleigh damping constitutes one of the convenient measures of damping that lumps the damping effects within the mass and stiffness matrices of the system. Rayleigh alpha is the parameter that determines the influence of the mass in the damping of the system. The higher the alpha value, the more the lower Frequencies is damped. Rayleigh beta is the parameter that determines the influence of the stiffness in the damping of the system. The higher the beta value, the more the higher frequencies are damped.

### 3.11 Water Conditions:

PLAXIS is generally used for effective stress analysis in which total stresses are divided into effective stresses,  $\sigma'$ , and active pore pressures,  $P_{\text{active}}$ .

$$\sigma = \sigma' + P_{\text{active}} \quad 3.24$$

Active pore pressure ( $P_{\text{active}}$ ) is defined as the effective saturation ( $S_{\text{eff}}$ ) times the pore water pressure,  $p_{\text{water}}$ .

$$P_{\text{active}} = S_{\text{eff}} \cdot P_{\text{water}} \quad 3.25$$

Water Pore pressure differs from active pore pressure when the degree of saturation is less than unity. PLAXIS can deal with the saturated soil below the phreatic level, as well as with partially saturated soil above the phreatic level.

In the pore water pressure a further division is made between steady state pore pressure,  $P_{\text{steady}}$ , and excess pore pressure,  $P_{\text{Excess}}$ .

$$P_{\text{water}} = P_{\text{steady}} + P_{\text{excess}} \quad 3.26$$

Excess pore pressures are pore pressures that occur as a result of stress changes in undrained materials. In this respect, changes in stress may be a result of loading, unloading, a change in hydraulic conditions or consolidation. Hence, excess pore pressures are a result of a deformation analysis. In a Consolidation analysis and a fully coupled flow-deformation analysis, excess pore pressures can occur in any material (except Non-porous materials), depending on the permeability as defined in the corresponding material data set.

# **CHAPTER FOUR**

## **MODELING PILE IN EXPANSIVE SOIL**

### **USING PLAXIS2D PROGRAM**

#### **4.1 General:**

The Demonstration Example for driven pile and the process of the driving piles in three sites in Khartoum city (Tuti Island Bridge, White Nile Bridge and Khartoum airport) was discussed in this chapter. PLAXIS2D software is used to models those piles in different soil layers.

The pile has a diameter of 0.5m for the three case studies, which represent the expansive soil and the diameter 0.4m for The Demonstration Example for driven pile.

The analysis process depends on information from geotechnical investigations were mainly performed by building and road research Institute and some other consulting firms (Al-Amery 2005) for the soil of three sites in Khartoum and the tutorial manual from the web site of PLAXIS for the Demonstrated example; also the default values from the PLAXIS2D software are used in these cases.

#### **4.2FEA Simulation for driving pile using PLAXIS 2D foundation:**

The simulation in PLAXIS 2D is performed by following steps

- Creation of geometry
- Generation of a finite element mesh
- Execution of a finite element calculation
- Evaluation of the output results



### 4.3 Building Geometry:

Firstly, PLAXIS 2D input program is started. New Project is chosen. The first step in every analysis is to set the basic parameters of the element model. This is done in the *General settings* window the default values are kept and in the *Dimensions* tab sheet, the default unit's boxes are kept:

Unit of Length = m      Unit of Force = kN      Unit of Time = s

In the Geometry Dimensions box the size of the required draw area is entered. Values for X left, X right, Y top, Y bottom. The spacing of snapping points can be further divided into smaller intervals by the Number of intervals value. Spacing and intervals are entered Figure: 4.1.

The screenshot shows the 'General settings' dialog box with the 'Dimensions' tab selected. The 'Units' section on the left has dropdown menus for Length (m), Force (kN), and Time (s). Below these, the units for Stress (kN/m<sup>2</sup>) and Weights (kN/m<sup>3</sup>) are displayed. The 'Geometry dimensions' section on the right contains input fields for Left (0.000), Right (30.000), Bottom (0.000), and Top (20.000), each with a unit of 'm'. The 'Grid' section below it has a 'Spacing' field (0.250) and a 'Number of snap intervals' field (1), both with units of 'm'. A 'Set as default' checkbox is located at the bottom left of the dialog. At the bottom right, there are three buttons: 'Next', 'OK', and 'Cancel'.

Figure: 4.1 Dimensions tab sheet of the General Settings window

For this project, the geometry is simulated by means of a xisymmetric model in which the pile is positioned along the axis of symmetry the general settings, the

standard Gravity acceleration is used ( $9.8\text{m/s}^2$ ) . Both the soil and the pile are modeled with 15-noded elements.

Figure 4.2 and Figure 4.3 show some information of White Nile Bridge model and also appendix A3 as example for entering data in the input program.

Figure: 4.2 Project tab sheet of the General Settings window

Once the general settings have been completed and confirmed, the drawing area appears with an indication of the origin and direction of the system of axes. The sub soil is divided into various thickness of different soil layer.

The pile is defined as column of 0.25m width for case studies piles and 0.2m for the Demonstration Example pile, The Interface elements are placed around the pile to model the interaction between the pile and the soil. The interface should be extended to about half ammeter under the pile tip; the interface should be defined only at the side of the soil. The boundaries of the model are taken sufficiently far away to avoid direct influence of the boundary conditions.

Standard absorbent boundaries are used at the bottom and at the right hand boundary to avoid spurious reflections.

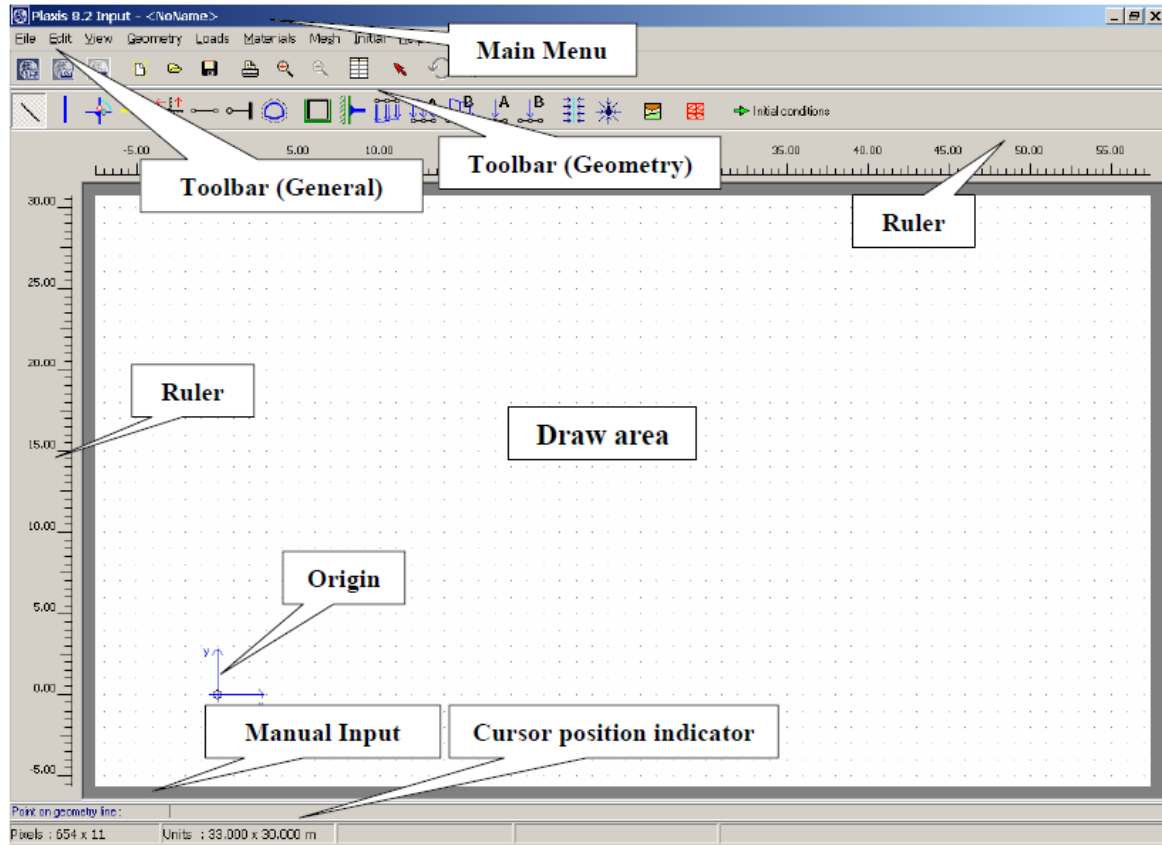


Figure: 4.3: main window of input program

#### 4.3.1 Dynamic loads:

in order to model the driving force a distributed unit load (system A) is created on top of the pile (from the loads menu) the creation and generation of dynamic load In the Input program:

Create loads such as loads system A or B and /or prescribed displacements set the appropriate load (loads system A) as a dynamic load using the Loads menu

#### **4.3.2 Material Data Sets:**

In order to simulate the behavior of the soil, a suitable material model and appropriate material parameters is assigned to the geometry. In PLAXIS, soil properties are collected in material data sets and the various data sets are stored in a material database. From the database, a data set is assigned to one or more clusters. PLAXIS2D FOUNDATION distinguishes between material data sets for soils and interfaces; the input of material data sets is done after the input of all geometry objects. Before the mesh is generated material data sets have assigned to all clusters and structures.

The input of material data sets is selected by means of the Materials button on the General Toolbar, from the options available in the Materials menu in the general tab sheet the material model, for this project the soil is modeled with the Mohr-Coulomb model. The behavior is considered to be Undrained (B). An interface strength reduction factor is used to simulate the reduced friction along the pile shaft.

In order to model the non-linear deformations below the tip of the pile in a right way, the short interface extend in the soil layer does not represent soil structure interaction. As a result, the interface strength reduction factors should be taken equal to unity (rigid).

The pile is made of concrete, which is modeled by means of the linear elastic model considering non-porous behavior. In the beginning, the pile is not present, so initially the soil properties are also assigned to the pile cluster.

For the Demonstration Example of driven pile which represent a concrete pile through an 11m thick clay layer into sand layer see Figures (A.1) and (A.2) of

appendix A1.where the properties of the soil and the concrete pile are listed in Table 4 .1 ,Tables 4.2, 4.3 and 4.4 for the case studies of White Nile Bridge, Tuti Island Bridge, Khartoum airport respectively

It should be noted that there is a remarkable difference in wave velocities between the soil and the concrete pile due to the large stiffness difference .This may lead to small time increments (many subs steps) in the automatic time stepping procedure.

This causes the calculation process to be very time consuming. Many sub steps may also be caused by a very small (local) element size. In such situations it is not always vital to follow the automatic time stepping criterion. The number of sub steps in the manual setting of the iterative procedure can reduced.

**Mohr-Coulomb - sandy silt**

General | Parameters | Interfaces

**Material set**

Identification: sandy silt

Material model: Mohr-Coulomb

Material type: UnDrained

**General properties**

$\gamma_{unsat}$ : 14.900 kN/m<sup>3</sup>

$\gamma_{sat}$ : 19.200 kN/m<sup>3</sup>

**Comments**

**Permeability**

$k_x$ : 0.000 m/day

$k_y$ : 0.000 m/day

Advanced...

SoilTest Next OK Cancel

Figure: 4.4 General tab sheet of the soil and interfaces data set window

**Table4:1 Soil and pile properties for the Demonstration Example  
for driven pile: (tutorial manual of Plaxis in Web Site of PLAXIS )**

Parameter	Symbol	Clay	Sand	Pile	Unit
Material model	Model	Mohr-C.	Hardening-S	Linear elast.	-
Type of behaviour	Type	Undrained	Undrained	Non-porous	-
Unit weight above phreatic line	$\gamma_{unsat}$	16	17	24	kN/m <sup>3</sup>
Unit weight below phreatic line	$\gamma_{sat}$	18	20	-	kN/m <sup>3</sup>
Young's modulus	$E_{ref}$	15000	50000	$3 \cdot 10^7$	kN/m <sup>2</sup>
Oedometer modulus	$E_{oed}$	-	50000	-	kN/m <sup>2</sup>
Power	$m$	-	0.5	-	-
Unloading modulus	$E_{ur}$	-	150000	-	kN/m <sup>2</sup>
Poisson's ratio	$\nu$	0.3	0.2	0.1	-
Reference stress	$P_{ref}$	-	100	-	kN/m <sup>2</sup>
Cohesion	$c$	2	1	-	kN/m <sup>2</sup>
Friction angle	$\varphi$	24	31	-	°
Dilatancy angle	$\psi$	0	0	-	°
Interface strength reduction	$R_{inter}$	0.5	1.0 (rigid)	1.0 (rigid)	-

**Table 4:2 Soil properties of White Nile Bridge (Al-Amery 2005)**

Parameter	Symbol	Pile	Silt clay	Clayey sand	Sandy clay	Unit
Depth	D	10	0 - 3.5	3.5 - 8.5	8.5-20	m
Material model	Model	Linear elastic	Mohr.C	Mohr.C	Mohr.C	-
Type of behavior	type	Non-porous	undrained	undrained	undrained	-
Unit weight above phreatic line	$\gamma_{unsat}$	25	14.8	-	-	KN/m <sup>3</sup>
Unit weight below phreatic line	$\gamma_{sat}$	-	18.9	19	20	KN/m <sup>3</sup>
Young modulus (constant)	$E_{ref}$	$3.10^7$	16100	17850	40000	KN/m <sup>2</sup>
Poisson's ratio	$\nu$	0.3	0.35	0.3	0.3	-
Cohesion	$C$	-	32.2	-	-	KN/m <sup>2</sup>
Friction angle	$\phi$	-	-	33.8	42	°
Interface strength reduction	$R_{inter}$	1.0riged	Manuel 0.5	1.0riged	1.0riged	-

**Table 4:3 Soil properties of Tuti Island bridge (Al-Amery 2005)**

Parameter	Symbol	Pile	Silty Clay	Silt	Unit
Depth	D	10	0 - 6.5	6.5 - 20	m
Material model	Model	Linear elastic	Mohr.C	Mohr.C	-
Type of behavior	type	Non-porous	undrained	undrained	-
Unit weight above phreatic line	$\gamma_{unsat}$	25	15.5	13.03	KN/m <sup>3</sup>
Unit weight below phreatic line	$\gamma_{sat}$	-	19.68	18.18	KN/m <sup>3</sup>
Young modulus (constant)	$E_{ref}$	$3.10^7$	26400	28300	KN/m <sup>2</sup>
Poisson's ratio	$\nu$	0.3	0.35	0.3	-
Cohesion	$c$	-	70.33	27.81	KN/m <sup>2</sup>
Friction angle	$\phi$	-	7.25	11.56	o
Interface strength reduction	$R_{inter}$	Riged 1.0	Manuel 0.5	Manuel0.5	-



**Table 4:4 Soil properties of Khartoum Air Port (Al-Amery 2005)**

Parameter	Symbol	Pile	Siltyclay	Clayely sand	Sandy clay	Unit
Depth	D	10	0 - 3.5	3.5 - 8.5	8.5-20	m
Material model	Model	Linear elastic	Mohr.C	Mohr.C	Mohr.C	-
Type of behavior	type	Non-porous	undrained	undrained	undrained	-
Unit weight above phreatic line	$\gamma_{unsat}$	25	14.8	-	-	KN/m <sup>3</sup>
Unit weight below phreatic line	$\gamma_{sat}$	-	18.9	19	20	KN/m <sup>3</sup>
Young modulus (constant)	$E_{inter}$	$3.10^7$	16100	17850	40000	KN/m <sup>2</sup>
Poisson's ratio	$\nu$	0.3	0.35	0.3	0.3	-
Cohesion	$c$	-	32.2	-	-	KN/m <sup>2</sup>
Friction angle	$\phi$	-	-	33.8	42	o
Interface strength reduction	$R_{inter}$	1.0riged	1.0riged	1.0riged	1.0riged	-

#### 4.4 Mesh Generation:

The mesh is generated using the default global coarseness (Medium) for the Geometry model of driven pile of White Nile Bridge as shown in Figure 4.5. The result of the Mesh generation is plotted in Figure 4.6.

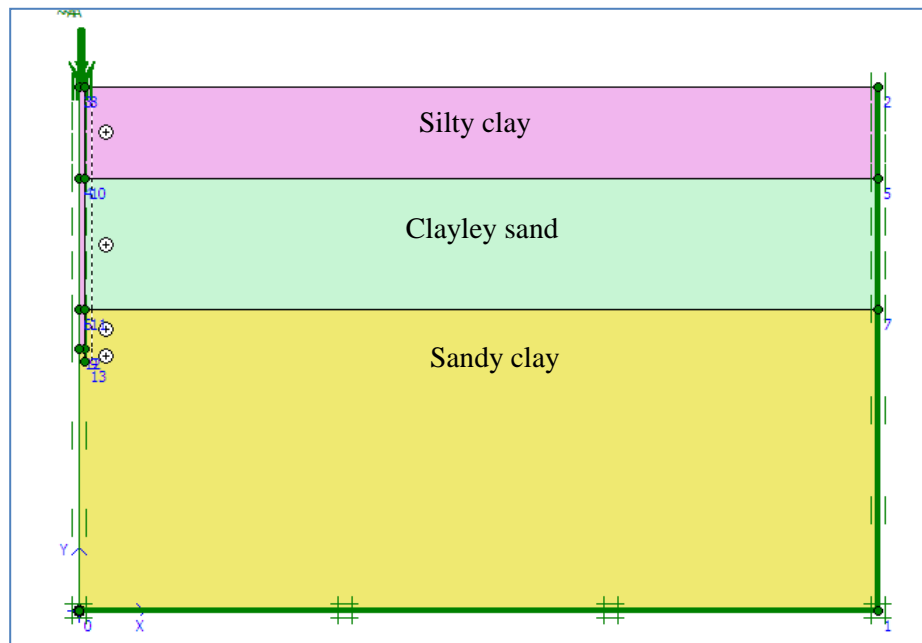


Figure 4.5 Geometry model of driven pile of White Nile Bridge

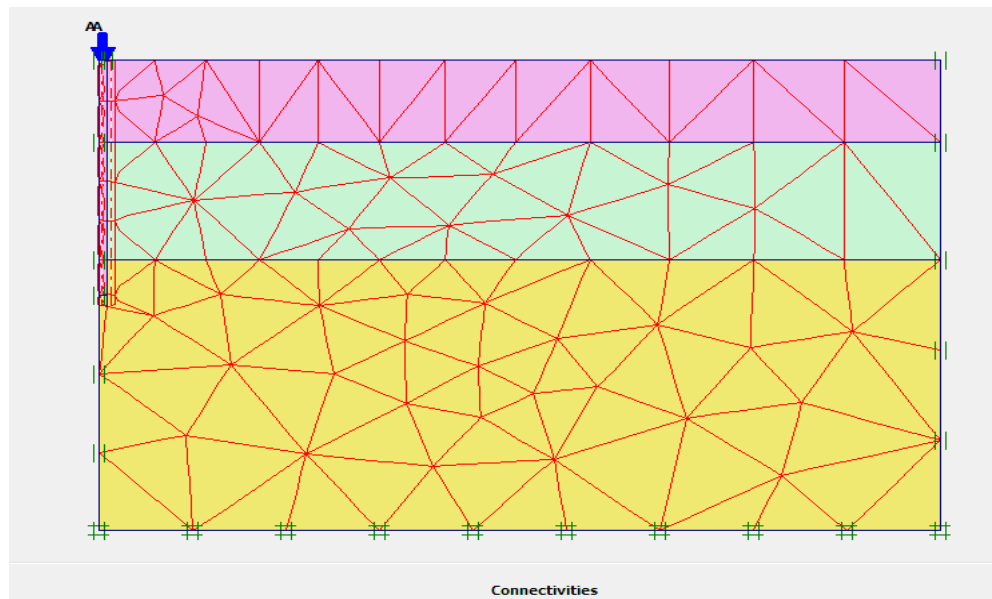


Figure: 4.6 .Finite element mesh for driving pile White Nile Bridge

#### **4.4.1 Initial Conditions:**

Before starting the actual calculations, the initial conditions must be generated. In general, the initial conditions comprise the initial geometry configuration and the initial stress state. These conditions are also taken into account to calculate the initial effective stress state. When a new project has been defined, a first calculation phase, named 'Initial phase', is automatically created and selected in the Phase list combo box and the Phases window if the phreatic level is assumed to be at the ground surface. Hydrostatic pore pressures are regenerated in the whole geometry according to this phreatic line. Initial phase and Initial effective stresses are generated by the K0 procedure, using the default values.

#### **4.5 Performing Calculation:**

Once the mesh has been generated, the finite element model is complete, and before the actual calculation is started, the calculation stages have been defined. The first of these is the definition of initial conditions. In the Initial phase, the initial stress conditions are generated. In the Phase1 the pile is created. In the Phase2 the pile is subjected to a single stroke, which is simulated by activating half a harmonic cycle of load system A. In the Phase3 the load is kept zero and the dynamic response of the pile and soil is analyzed in time. The last two phases involve dynamic calculations.


##### **4.5.1 Phase One:**

- Click Next to add a new phase.
- Select Plastic option in the General tab sheet.
- The Staged construction option is by default selected in the Parameter tab sheet
- Click Define Assign the pile properties to the pile cluster.

- Activate the interface and the dynamic load at the top of the pile. The Dynamic load will be considered in the Dynamic calculation in the next phase.

#### 4.5.2Phase Two:

- Click Next to add a new phase.
- Select Dynamic in the General tab sheet.
- Use standard Additional steps (100)
- Reset displacements to zero.
- Enter 0.01 S for the Time interval.

In the Multipliers tab sheet click  next to Load system A to apply the dynamic loading. Define the dynamic loading by entering the values as indicated. Figure 4.7 illustrates Dynamic loading parameters the result of this phase is half a harmonic cycle of the external load in system (A), at the end of this phase, the load is back to zero.

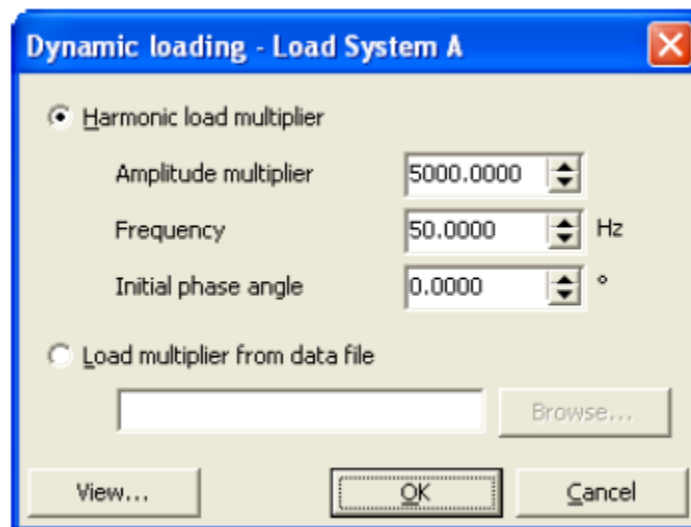


Figure: 4.7Dynamicloadingparameters

#### 4.5.3Phase Three:

- Select Dynamic in the General tab sheet.
- Use standard Additional steps (100).

- Enter a Time interval of 0.19 s.
- In the Multiplier tab sheet, all multipliers remain at their default values. Click the button next to Load system (A), in the Dynamic Loading window set all parameters to zero and select point node at the top of the pile for load displacement curves. After the definition of the phase's Figure 4.8 the Calculation command is given. Then the calculation took several minutes to perform the calculation Figure 4.9. When a calculation ends, the window is closed and focus is returned to the main window.

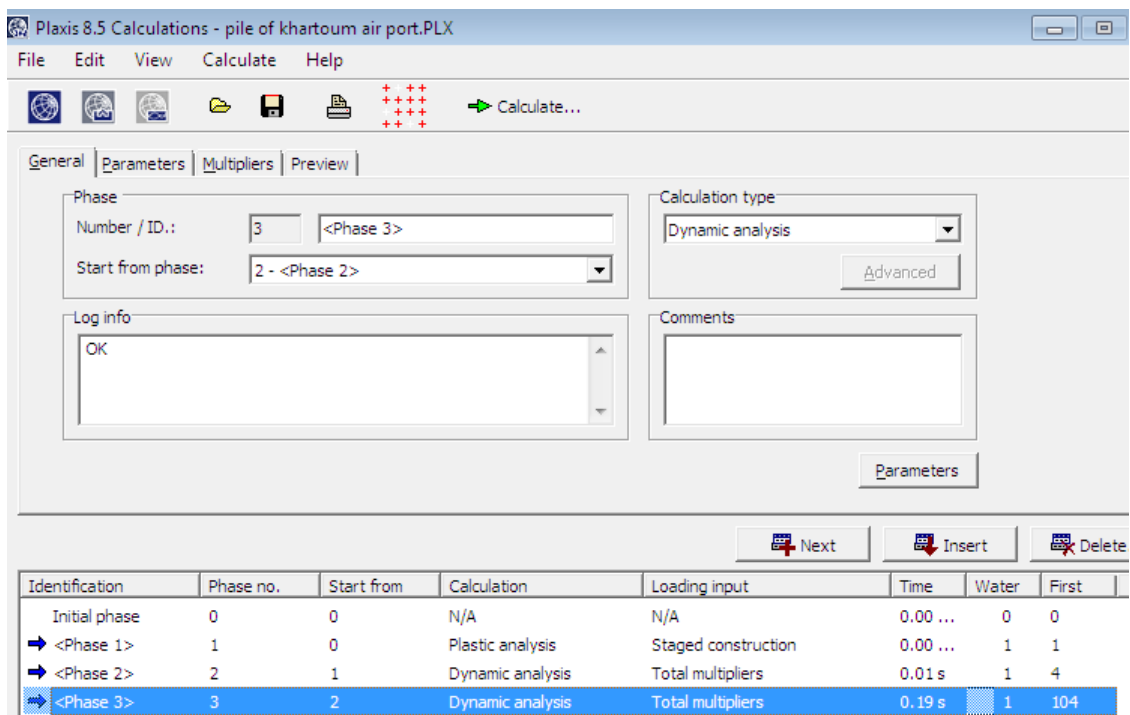


Figure: 4.8 the definition of the phases

## 4.6 Viewing Output Results:

The main output quantities of finite element calculation are the displacements at the nodes and stresses at the stress points. When a finite element model involves structural elements, structural forces are calculated in these elements. An extensive range of facilities exist within PLAXIS to display

the result of finite element analysis. Once the calculation has been completed, the results are evaluated in the Output program, the displacement and

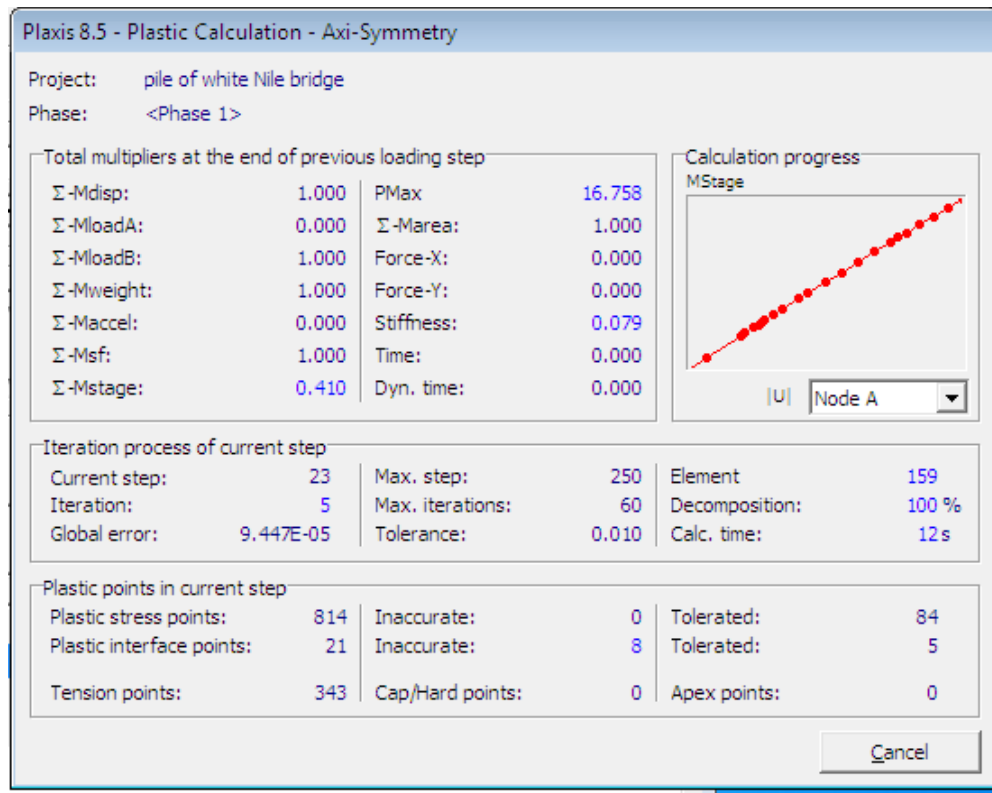


Figure: 4.9 perform the calculation

stresses are viewed in the full2D model as structural elements, to documented project input data and result , a Report generation facility is available in the output program also the Dynamics module provides special options to display the results of the Dynamic analysis.

With the menu option Create Animation in the View menu it can actually see the motion of the geometry in a time. The number of steps in the animation can be influenced by the number of additional steps defined in the calculation phase as illustrated in Figure 4.10. For dynamic steps several velocity and acceleration options are available in the Deformations menu. It can be selected the total velocities, the total accelerations, the horizontal components and the vertical

components. For the use of the Curves program of PLAXIS with the dynamic analysis module can display the velocity or acceleration as well as displacements as a function of time, Plots of time versus displacements, velocities, accelerations or multiplier can be displayed Figure 4.11.

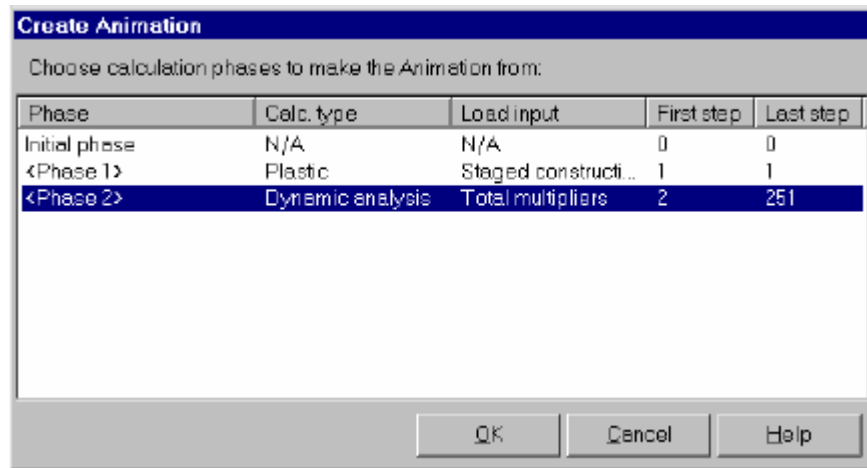


Figure: 4.10 selection of phase from create animation window

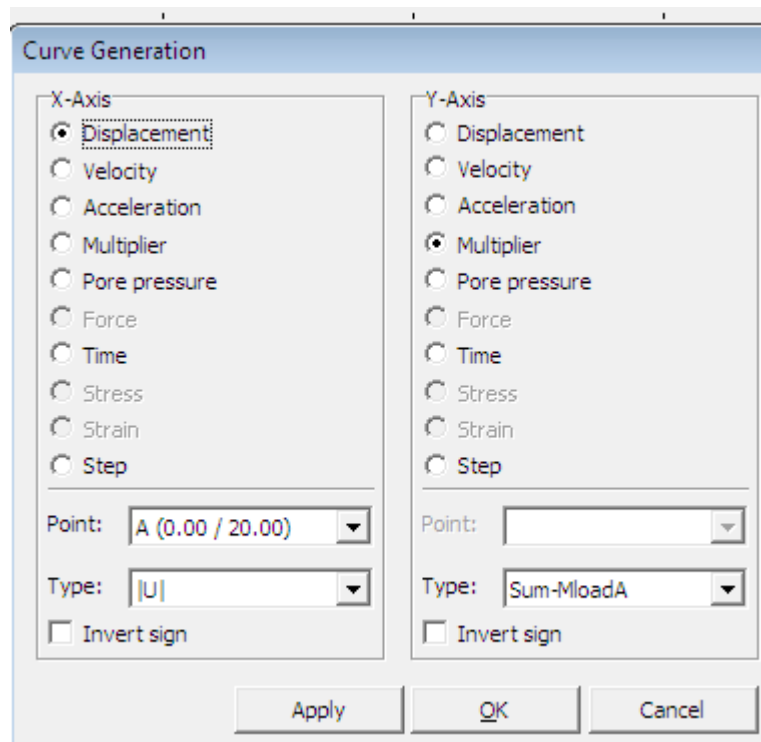


Figure 4.11 Dynamic fields in curve generation window

# CHAPTER FIVE

## ANALYSIS AND DISCUSSION OF RESULTS

### 5.1 Introduction:

The results of the numerical analysis are presented in this chapter, and the focus is placed on the irreversible deformations below the pile and the adjacent soil due to the driving process.

### 5.2 Demonstration Example for driven pile:

Figure (5.1) shows the settlement of the pile (top point) versus time. From this Figure the following observations can be made:

- The maximum vertical settlement of the pile top due to this single stroke is about 0.115mm. However, the final settlement is almost 0.110mm.
- Most of the settlement occurs in phase 3 after the stroke has ended.

This is due to the fact that the compression wave is still propagating downwards in the pile causing additional settlements.

- Despite the absence of Rayleigh damping, the vibration of the pile is damped due to soil plasticity and the fact that wave energy is absorbed at the model boundaries.

The influence of excess pore pressures which reduces the shear strength of the soil illustrated in Appendix A2 and Figure 5.2 shows the shear stresses in the interface elements at  $t=0.01s$ , the plot shows that the maximum shear stress is reached all along the pile, which indicates that the soil is sliding along the pile.



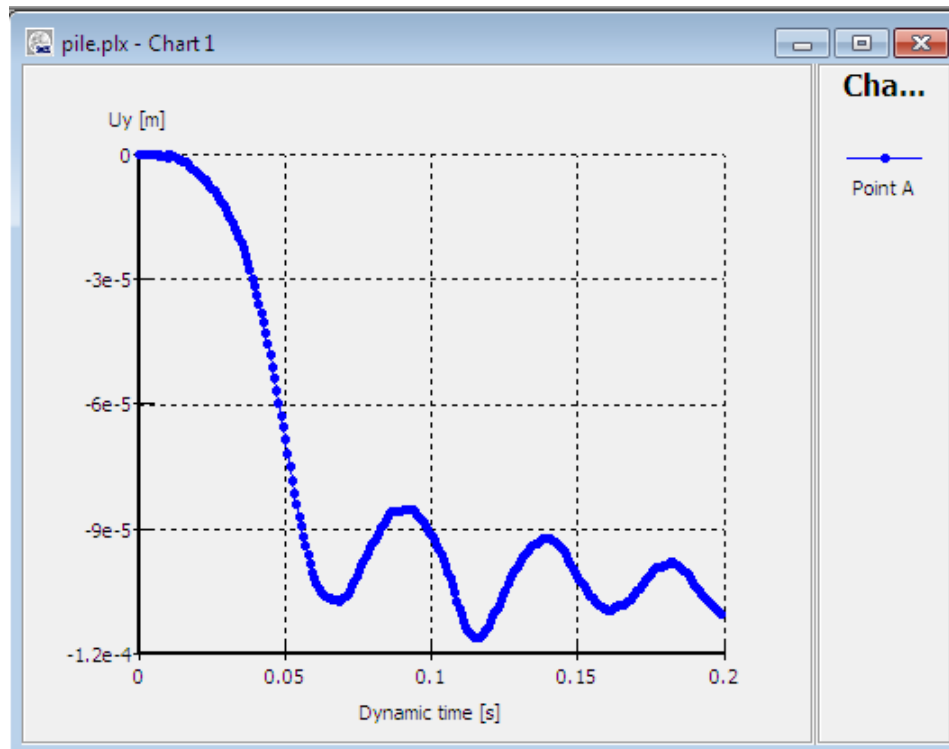


Figure 5.1 Pile settlements vs. time for Demonstration Example for driven pile

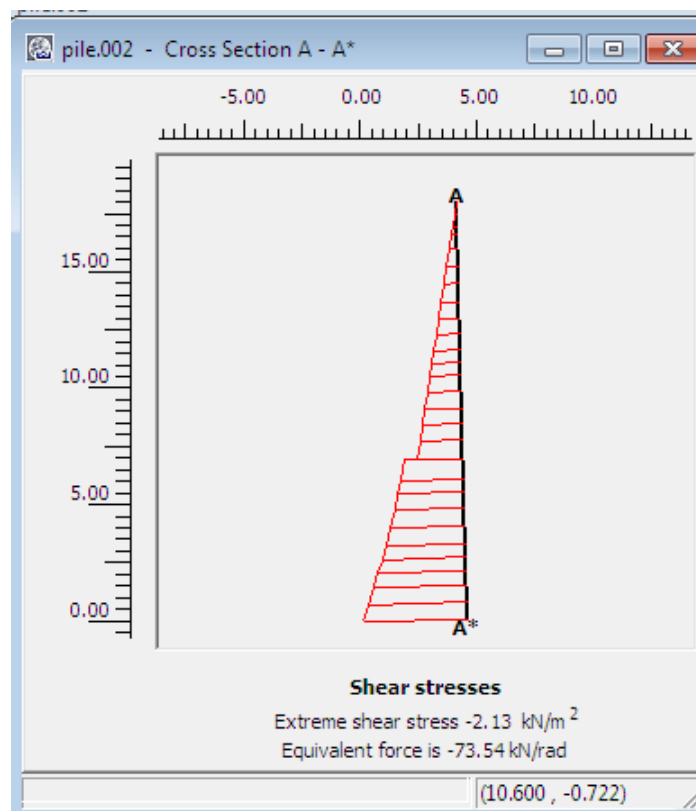


Figure 5.2 the shear stresses in the interface elements at  $t = 0.01$  s

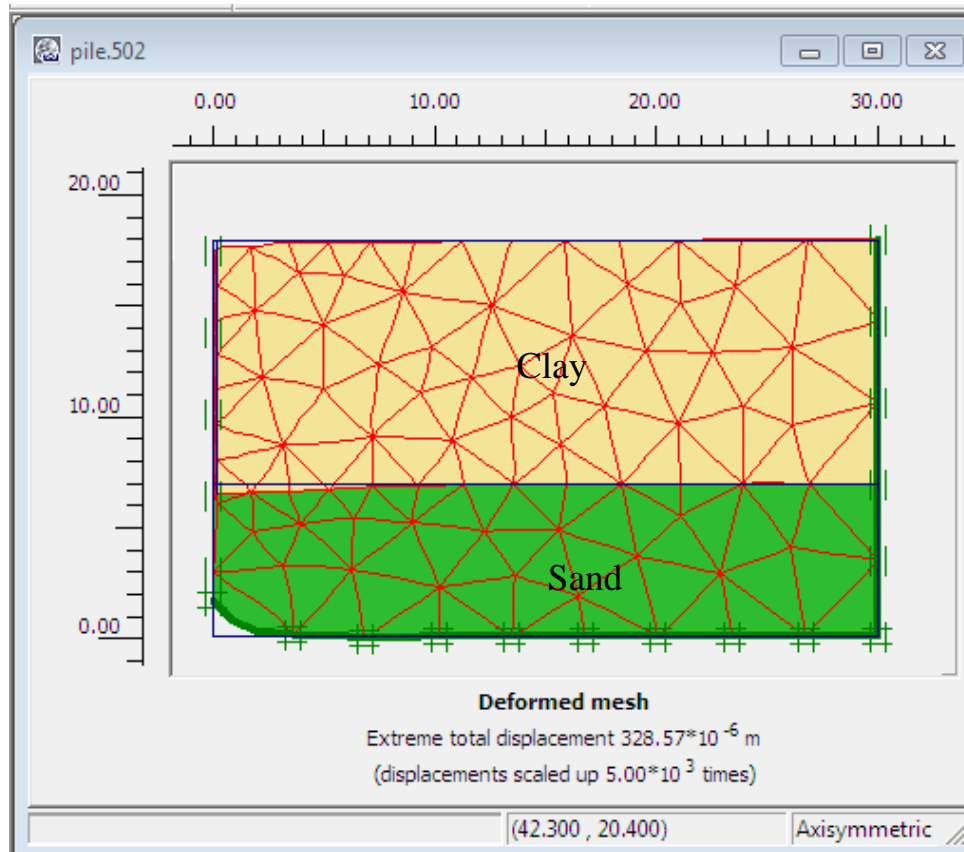


Figure 5.3 the deformed mesh of the last calculation phase

### 5.3 The pile of White Nile bridge area:

- As can be seen from Figure 5.4 the shear stresses in the interface elements at  $t=0.01s$  The plot shows that the maximum shear stress is reached all along the pile, which indicates that the soil is sliding along the pile at the beginning of the process of the driving pile. But from Figure 55, the output of the second calculation phase ( $t=0.01s$ ) just after the stroke), it can be seen that large excess pore pressures occur in the layer of sandy clay soil .This cause soil settlement of the soil layers around the pile where is represent one of serious problem in expansive soil during the driving pile process.

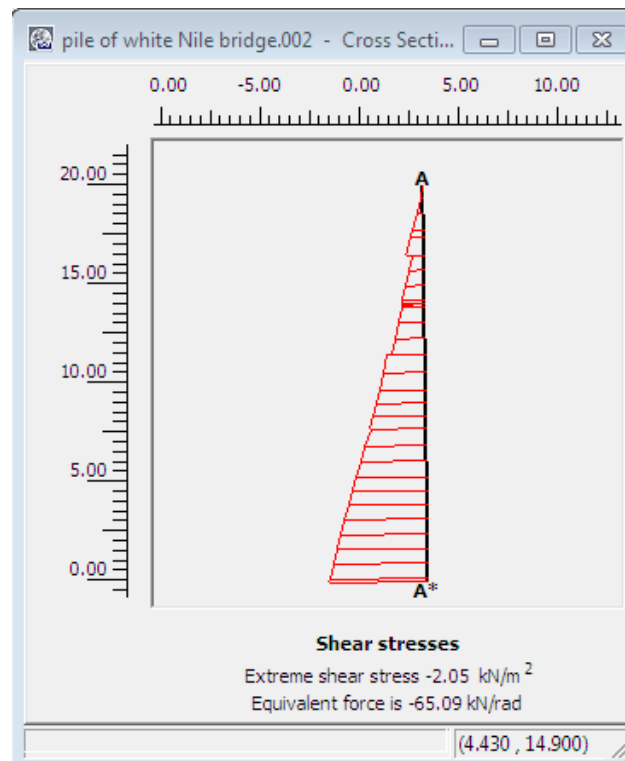


Figure 5.4 the shear stresses in the interface elements at  $t=0.01s$

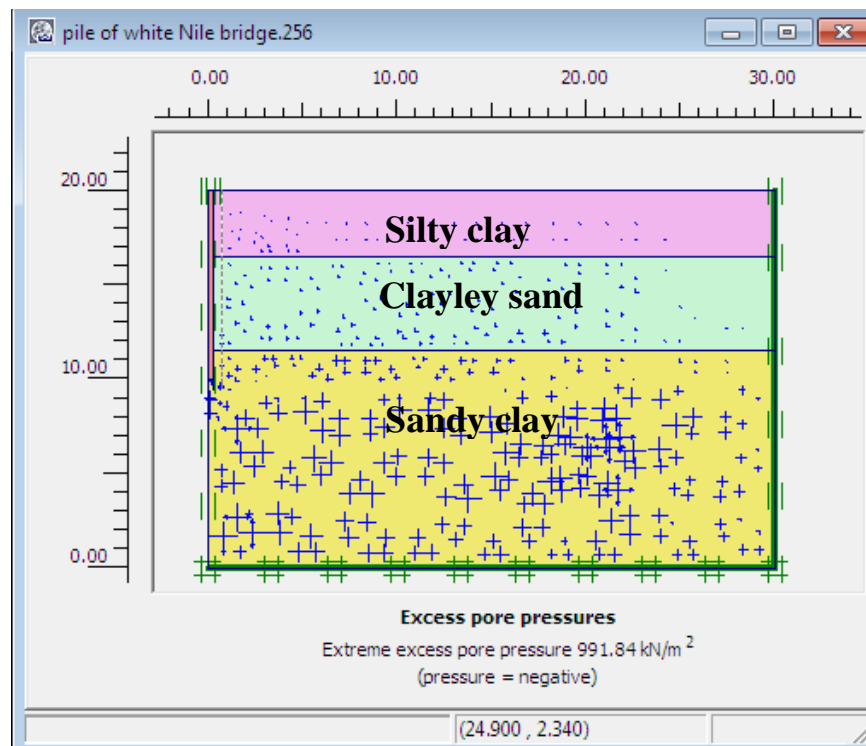


Figure 5.5 the output of the second calculation phase

- From Figure 5.6 which represent the plot of the settlement of the pile (top point) versus time, it can be seen that The final vertical settlement of the pile top due to this single stroke is about 17mm, also it can be observed that most of the settlement occurs in phase 3 after the stroke ended.

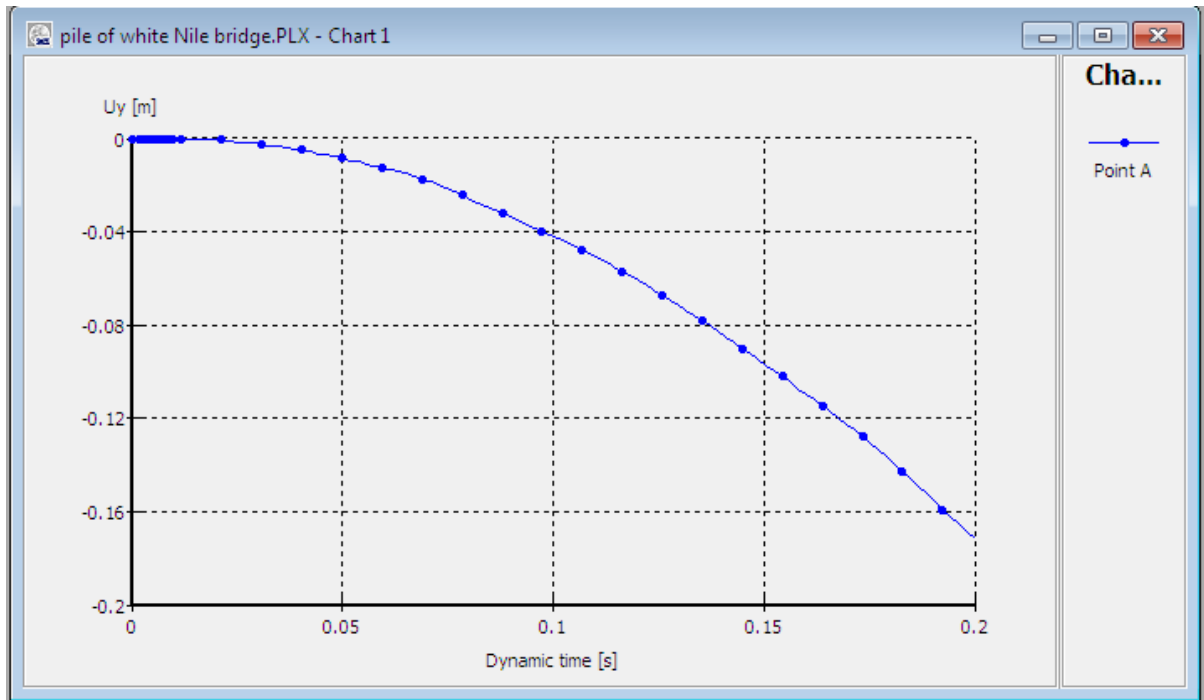


Figure 5.6 pile settlement vs. time for White Nile bridge area

- Figure 5.7 represent the deformed mesh of the last calculation phase ( $t=0.2s$ ), this Figure and table 5:1 demonstrated the final settlement of the pile and the adjacent soil layers.
- The settlement of the adjacent soil layers represents problem according to the Korean Society of Architectural Engineers (2004), and it can be reduced with the certain controlling procedure before the driving process as stated in section (2.5.8)

Table 5:1 the value of the settlements for the pile and the soil of White Nile Bridge at selected nodes at surface

Plaxis 8.6 Output - [pile of white Nile bridge.502 - Soil element displacements]						
File Edit Deformations Stresses Geometry Window Help						
Node	X [m]	Y [m]	Ux [10 <sup>-3</sup> m]	Uy [10 <sup>-3</sup> m]	ΔUx [10 <sup>-6</sup> m]	ΔUy [10 <sup>-6</sup> m]
27	0.000	20.000	0.000	-167.345	0.000	-67.417
253	5.728	20.000	-5.842	-160.916	-2.480	-67.724
395	10.000	20.000	-10.132	-159.773	-5.138	-66.214
575	15.510	20.000	-17.102	-154.497	-2.673	-64.829
843	20.341	20.000	-20.291	-140.804	-6.946	-56.396
995	25.772	20.000	-18.218	-115.766	-5.194	-53.459
1046	30.000	20.000	-8.997	-95.625	-4.035	-42.514

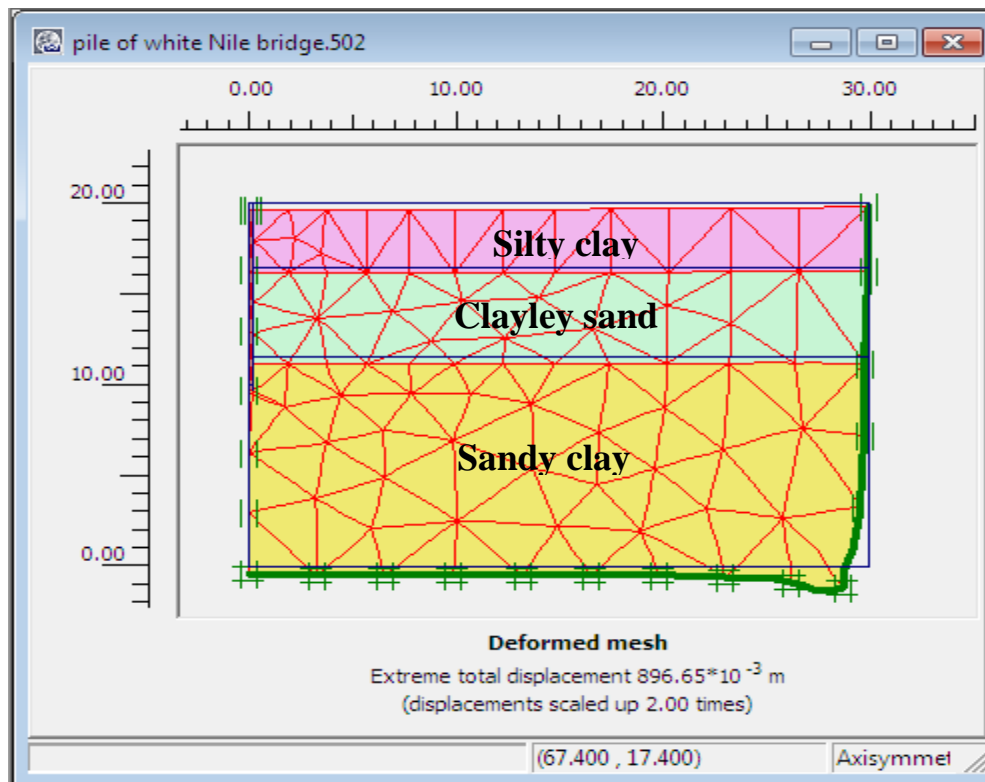


Figure 5.7 The deformed mesh of the last calculation phase

## 5.4 The Pile of Tuti Island bridge areas:

- Figure 5.8 shows the shear stresses in the interface elements at  $t=0.01s$ , also the plot Shows that the maximum shear stress is reached all along the pile, which indicates that the soil is sliding along the pile at the binging of the dynamic process of the driving pile.

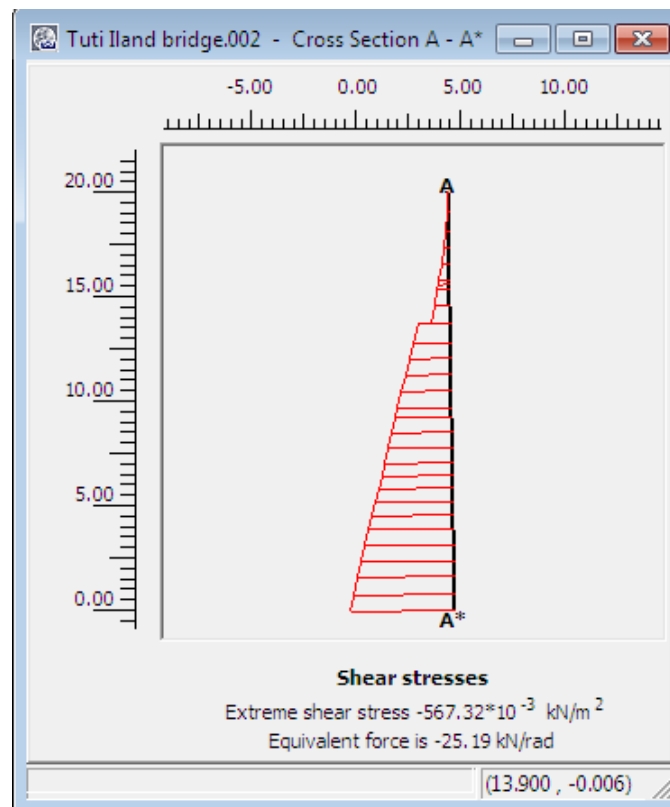


Figure 5.8 the shear stresses in the interface elements at  $t=0.01s$

From Figure 5.9 and Table 5.2 which represented the displacement of the pile (top point) versus time. it can be seen that the pile is heaved due to driving process about 0.0256mm also it can be seen that from figure 5.10, but this value does not make significant problem as described in the (Massachusetts State building code and project specifications), piles identified with vertical displacement exceeding 1.3 cm required redriving

Table 5:2 the value of the heave for the pile and the soil of Tuti Island  
Bridge area at selected nodes at surface

Plaxis 8.6 Output - [Tuti Island bridge.502 - Soil element displacements]						
File Edit Deformations Stresses Geometry Window Help						
Node	X [m]	Y [m]	Ux [10 <sup>-6</sup> m]	Uy [10 <sup>-6</sup> m]	ΔUx [10 <sup>-6</sup> m]	ΔUy [10 <sup>-6</sup> m]
79	0.000	20.000	0.000	25.571	0.000	0.609
325	5.243	20.000	2.733	4.680	0.121	0.146
653	10.000	20.000	2.961	4.685	0.038	0.120
965	15.510	20.000	1.920	2.195	0.036	0.058
1173	20.341	20.000	1.269	1.692	0.001	0.012
1281	25.772	20.000	0.599	1.247	0.010	0.017
1368	30.000	20.000	0.241	1.043	0.003	0.028

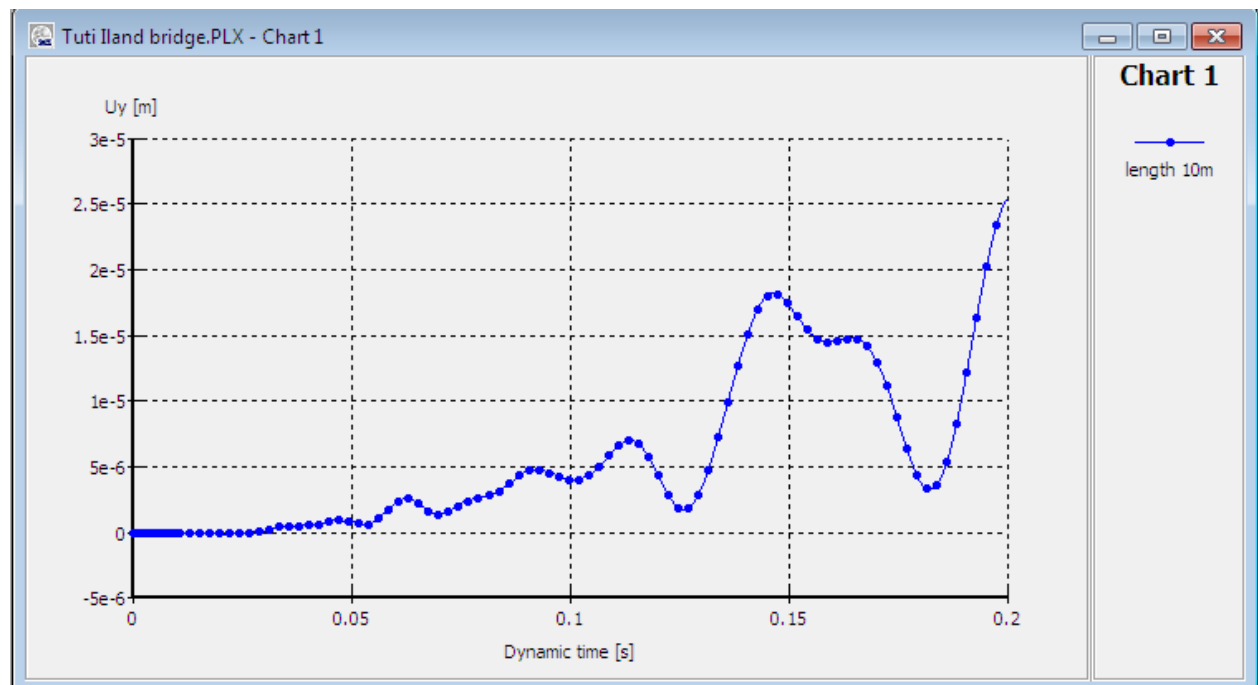


Figure 5.9 the displacement of the pile for the Tuti Island bridge area

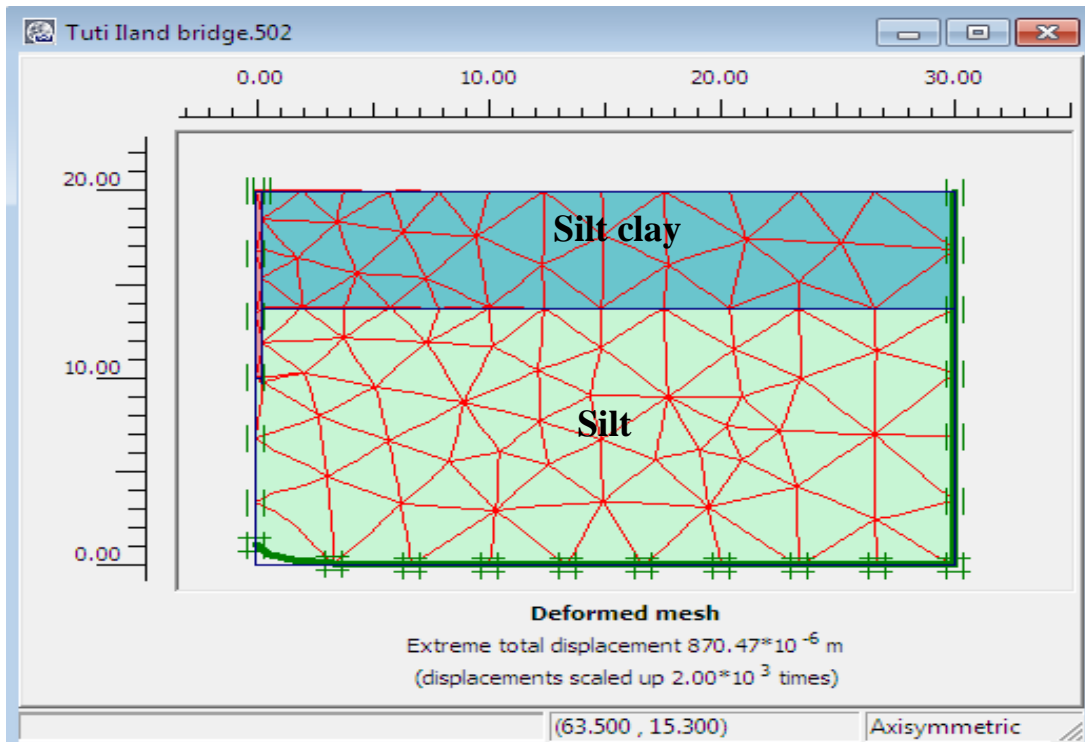


Figure 5.10 the deformed mesh of the last calculation phase

## 5.5 Comparison with different length of driven pile:

The result of driving pile with a different length which was shown in Figure 5.11 and 5.12 show that settlement of the pile top point and the heave of pile due to driving pile process is increasing due to increase of the pile length in the

Table 5:3 the value of the settlements and the heaves

Pile length (m)	6m	10m	16m
Settlement in White Nile (mm)	161	168	180
Heave of pile in Tuti Island (mm)	0.0018	0.0025	0.0039



Area of the White Nile Bridge and Tuti Island Bridge which is represent the expansive soil.

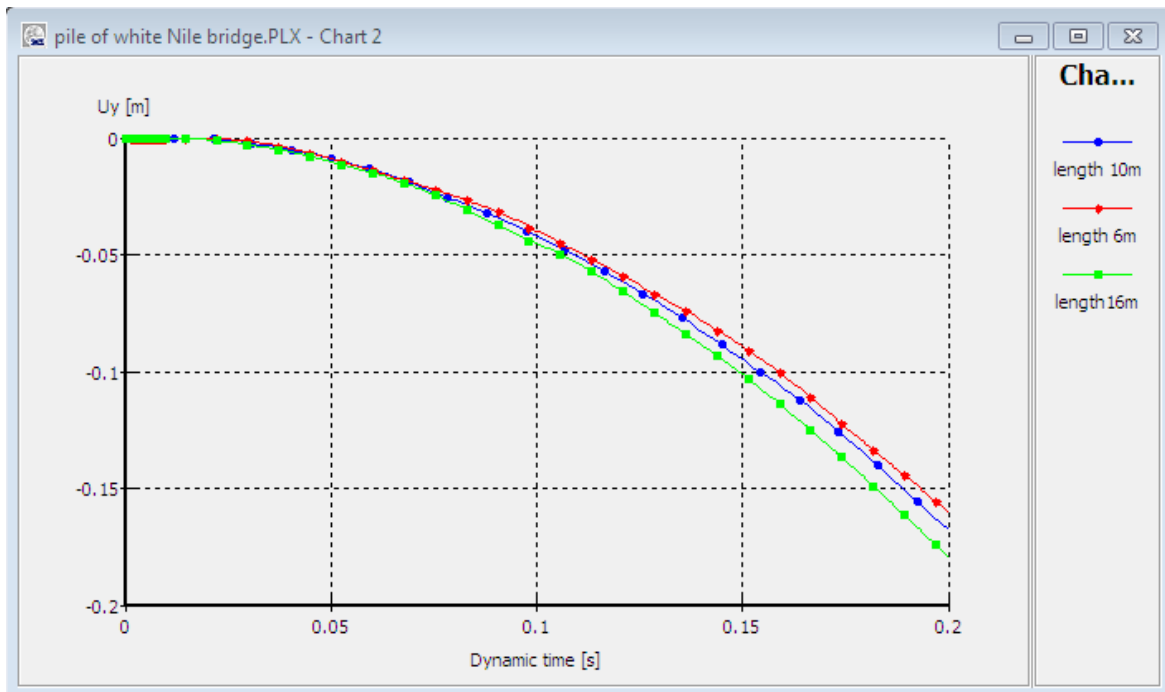


Figure 5.11 the settlements due to driving pile for different lengths

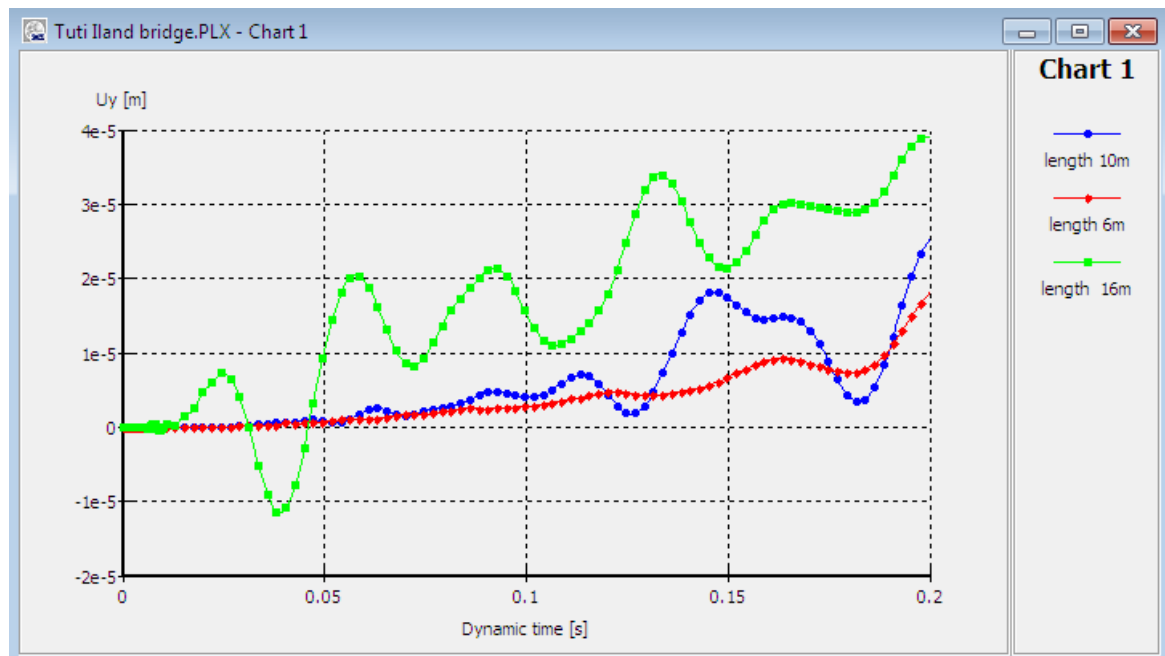


Figure 5.12 the heaved piles due to driving pile for different lengths

## 5.6 The Pile of Khartoum Air Port Area:

(Accuracy condition not reached in last step Maximum number of iteration reached) this message which was reported in the calculation tab sheet in (log information) as shown in Figure 5.16 , this model needs more investigation to demonstrate this reporting message, because the reason for this result was not clear. Figures A.7 and A.8 from appendix A4, shows the displacement and the deform mesh of Khartoum airport respectively

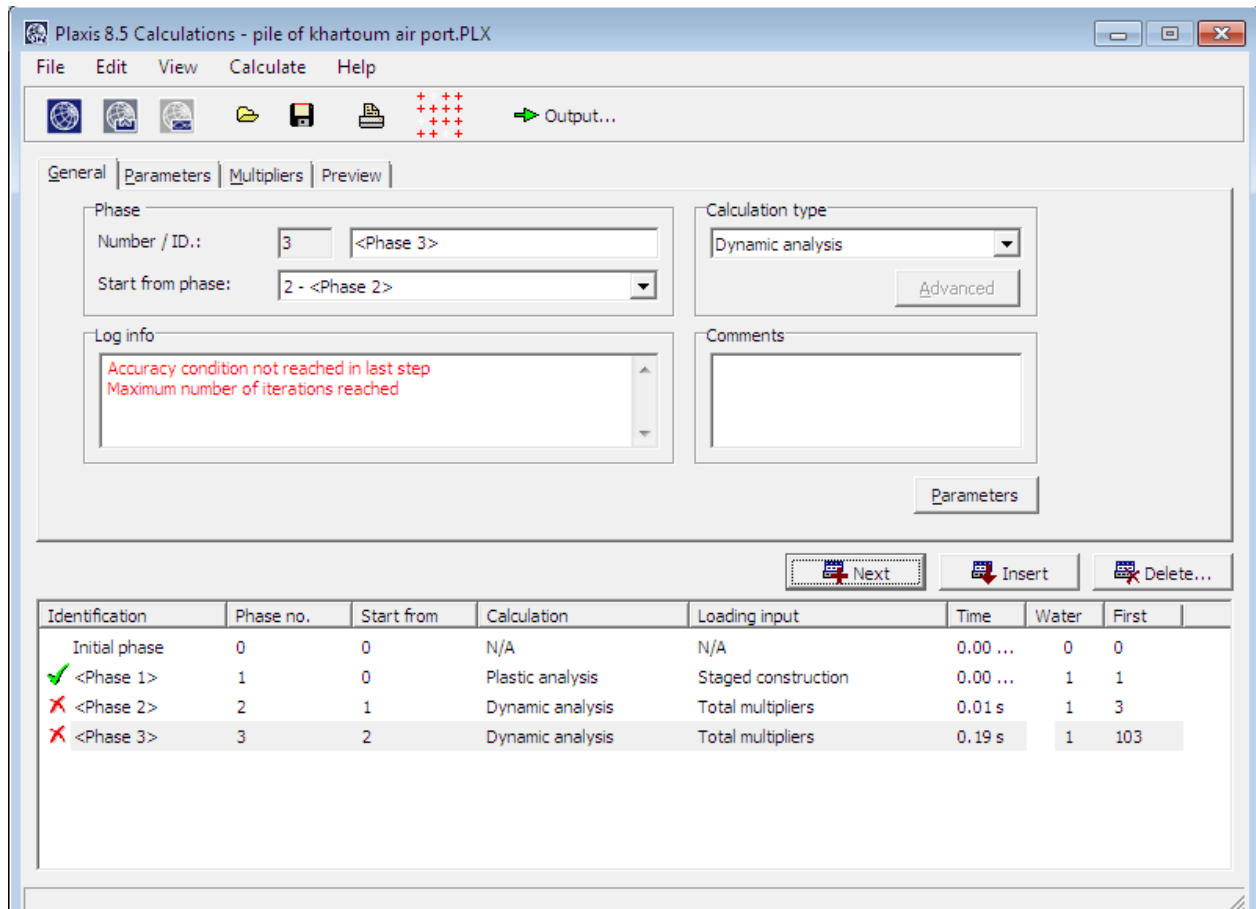


Figure 5.13 the result of calculations of the phases of Khartoum air port

# CHAPTER SIX

## CONCLUSIONS AND RECOMMENDATIONS

### 6.1 Introduction:

The present study illustrates the possibility of simulating the mechanical behavior of expansive soil using the finite element method with Mohr coulomb and Harding soil models. A numerical simulation of a driven pile in expansive soil has been carried out.

### 6.2 Conclusions:

From this study it was concluded that:

- The possibility of simulating the behavior of the driven pile in expansive soil by using the finite element method and this study gives Comprehensive understanding of the finite element program PLAXIS 2D Foundation software.
- Also this study demonstrated that the Finite Element Analysis is an appropriate method to determine the effect of the driving pile process in expansive soil.
- The model which represents the driven pile in Khartoum airport area did not satisfied the accuracy condition at the last step of the calculation phase and the reason was not clear for this result.
- The model which represents the driven pile of Khartoum airport area needs more investigation to demonstrate the reasons that led to the failure to achieve the accuracy condition of model in this study.
- Through this study, the presences of some phenomena related with the driving pile process in expansive soil was observed, The first phenomena is the settlement of the soil adjacent the pile which represents problem as in

appendix A3, but it can be reduced by a certain procedure before the process of the driving pile as stated in section (2.5.9). The second phenomenon represents heave of the pile due to the dynamic process, but it does not make a significant problem as stated in section (5.3).

- Also it can be observed that the length of the pile is a significant factor for this phenomenon because the increase of pile length increases the settlement in the expansive soil and the heave of the pile.

### **6.3 Recommendations:**

For future studies it is recommended that:

- To use other model such as the Soft Soil creep model for the driven pile of Khartoum airport which needs more investigation.
- Also it is recommended to use a more advanced Hardening soil model just for the sand layer and Mohr Coulomb for all types of clay layer in expansive soil in Khartoum location and compare results with results of this study.
- Modeling of pile groups and the effect of the driving process on the piles group interaction also should be investigated.
- The influence of the driven pile close to an existing building should be studied.

## **References:**

1. Abed Ayman, 2008, "Numerical Modeling of Expansive Soil Behavior" H.R .Thesis, university of Institutes fur Geotechnical, Stuttgart.
2. Ahmed, Sa'ad A -Wahab, 1989, "Dynamic analyses of pile driving", H.R .Thesis, Department of Civil Engineering, University of Glasgow.
3. Al-Amery, Mukdad Mahmod, 2005, "Analysis and Design of Piles in Central Khartoum Using Finite Element Method", M.sc .Thesis, College of Graduate Studies, Sudan University of Science and Technology.
4. Bell, R., Davie, R., Clemente, L. and Garland, 2003, "Proven Success for Driven Pile Foundations", Cleveland, Ohio; garland@pile.com.
5. Bosscher, Peter J. "Pile & Pier Foundation Analysis & Design", University of Wisconsin-Madison.
6. Bowles, Joseph E., 1997 "Foundation Analysis and Design" Fifth Edition P.E., S.E.Consultant Engineering Computer Software Peoria, Illinois.
7. Bureau of Bridges and Structures "Pile Foundation Construction Inspection Class", Reference Guide, at:<http://www.dot.il.gov/bridges/geotechtraining.html>.
8. Deeks John, 1992, "Numerical Analysis of Pile Driving Dynamics", H.R .Thesis, the University of Western Australia, Department of Civil Engineering .
9. El Bdawy El Sayed, R.A, Salem, T. N.and El Sakhawy, N.R ,2016, "Pile Behavior in Expansive Soil". The International Conference of Engineering Science and Application, Aswan, Egypt.
- 10.Foundation and Civil Engineering Site Development", Engineering Hand Book, Downloaded from, Digital Engineering Library @ McGraw-Hill.

- 11.Hekmat,Zulkifli , Mohammad hossein and Roozbeh ,2012, “Three Dimensional Dynamic Analysis of Interaction Soil-Pile with Coupling Finite Element Analysis (FEA) and Boundary Element Method (BEM)” , Master Student of Construction Management, AWAM International Conference on Civil Engineering &Geohazard Information Zonation.
- 12.Holt, M.I. and McVay, M. (1994). “LPGSTAN User's Manual”. University of Florida, Gainesville.
- 13.Hussein ,M.H and,Sheahan, J.M. ,1993 ,“Uplift capacity of driven piles from static loading tests”, Pittsburg, Pennsylvania .
- 14.Jalali, Reza and Alistair, 2012, “Using Finite Element method for Pile-Soil Interface (through PLAXIS and ANSYS)” , 2012, Journal of Civil Engineering and Construction Technology. Available online at <http://www.academicjournals.org/JCECT>
- 15.Kim, S.R., Chung, G.O., Ngyen, T.D., and Fellenius, B.H., 2012."Design for Settlement of GroupsofPile”, by the Unified Design Method”, Korea.
- 16.Lsmer J. Kuhlmeier R.L.(1969) “Finite Dynamic Model for InfiniteMedia” ASCEJ.of the ENg.
- 17.Masoum-, G., 2005, “Numerical modeling of free field vibrations due to pile driving using a dynamic soil-structure interaction formulation”, H.R .Thesis, Degrande\_, Department of Civil Engineering.
- 18.Mehmet, Rodrigo, P.E. and Svinkin, Mark R., “Evaluation of Vibrations and Limits and Mitigation Techniques for Urban Construction” Youngcheol Kang, Cleveland, Ohio.
- 19.NELSON ,2015, “Modelling of negative skin friction on bored piles in clay” Department of Civil and Environmental Engineering Division of GeoEngineering Geotechnical Engineering, Chalemrs University of Technology Goteborg, Sweden.

20. Nordlund, R.L., (1963), "Bearing Capacity of Piles in Cohesionless Soils" American Society of Civil Engineers,
21. Office of Infrastructure Research and development, 2006, "Design and Construction of Driven Pile Foundation", U.S. Department transportation Federal Highway Administration Georgetown Pike McLean.
22. PLAXIS2D scientific Manual, material model Manual, reference Manual, tutorial Manual 2012.
23. Sithharam, T, G, 2013 "Advanced Foundation Engineering", Indian Institute of Science ,Bangalore.
24. The Government of Hong Kong Special Administrative Region, 2004 "Code of practices' for foundation", Prepared by: Buildings Department, Mongkok, Kowloon Hong Kong.
25. Tomlinson, M.J, 1994, "Pile design and construction practice" fourth edition.
26. Zienkiewicz, O. C, 1989, "The Finite Element Method", 4th edition, Mc Graw-Hill, London.

## APPENDICES

### Appendix A1

This figure demonstrate the soil profile and Situation of the pile for demonstration example

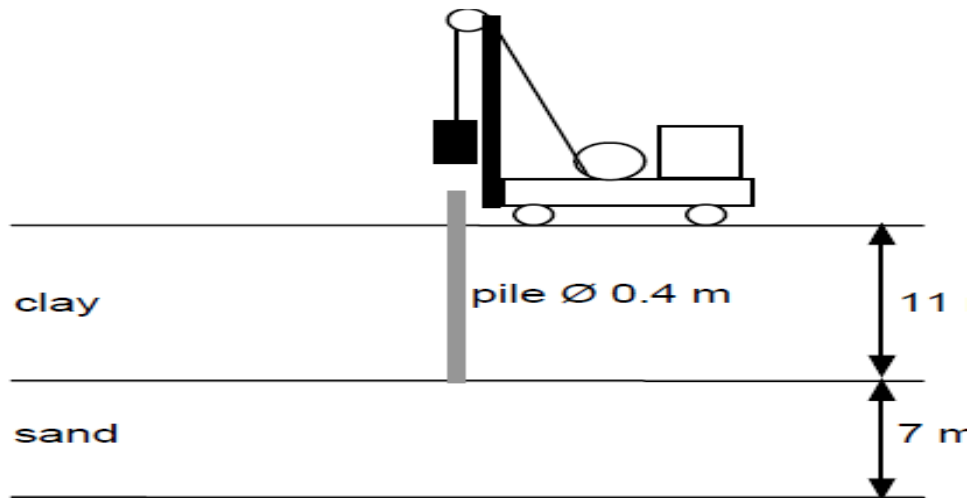


Figure A.1 The Demonstration Example of pile driving

And this figure demonstrate the interface elements, standard fixities and absorbent boundaries in the geometry model

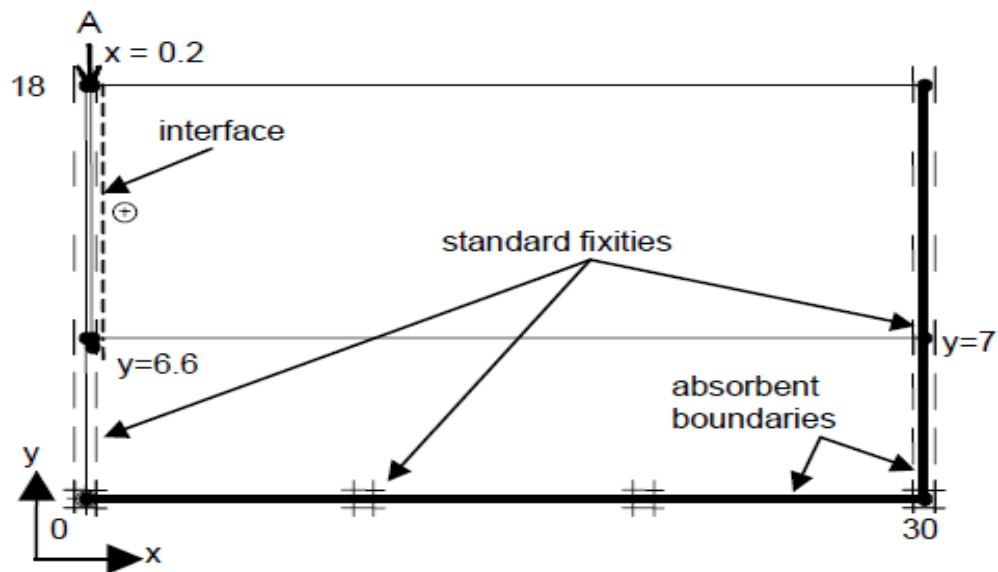


Figure A.2 geometry model for the Demonstration Example



## Appendix A2

The influence of Excess pore pressures:

Excess pore pressures are pore pressures that occur as a result of stress changes in undrained materials it can be included in the analysis if undrained soil behavior is assumed

PLAXIS Program has a series of advantages:

- Excess pore pressure: Ability to deal with excess pore pressure phenomena. Excess pore pressures are computed during plastic calculations in undrained soil.
- Soil-pile interaction: Interfaces can be used to simulate intensely shearing zone in contact with the pile, with values of friction angle and adhesion different to the friction angle and cohesion of the soil

The influence of excess pore pressure appear at Figure (A.2) which represent the output of the second calculation phase of the Demonstration Example at ( $t=0.01s$ ) just after the stroke), it can be seen that large excess pore pressures occur very locally around the pile tip. This reduces the shear strength of the soil and contributes to the penetration of the pile in to the sand layer. The excess pore pressures remain also in the third phase since consolidation is not considered.

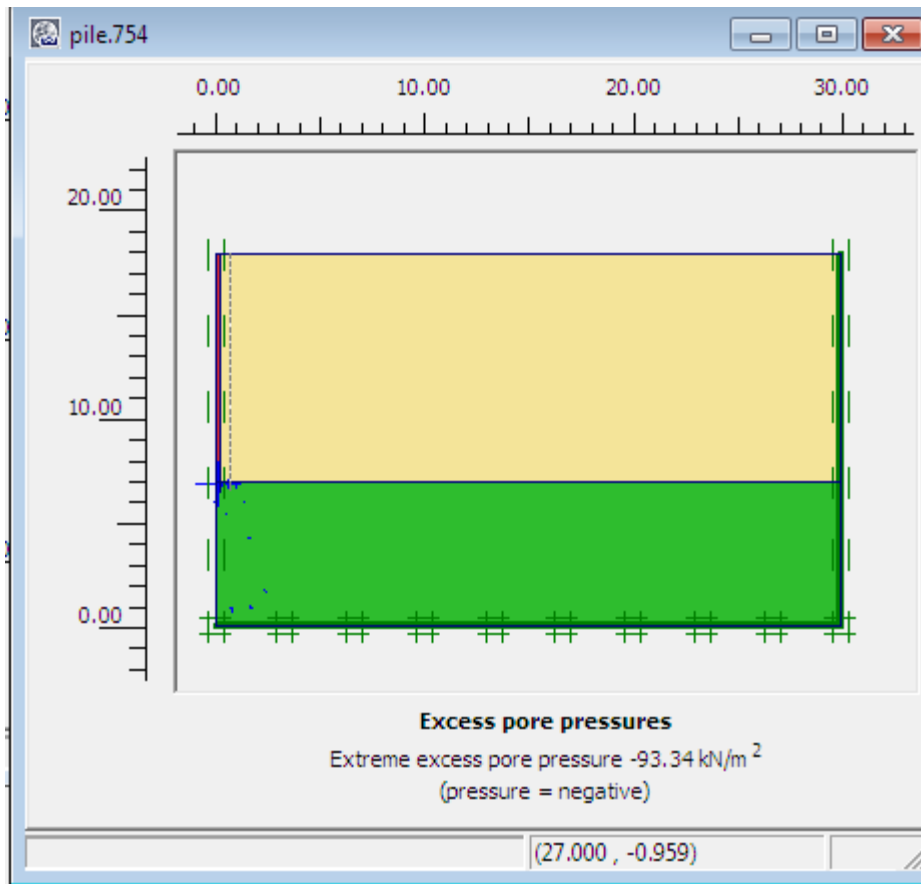


Figure A.3 the output of the second calculation phase

## Appendix A3

The input data and information of the pile of White Nile Bridge from the output program

**General info**

Project

Filename : pile of white Nile bridge

Directory : D:\Users\Mahdi\Desktop\

Title : pile of white Nile bridge

General options

Model : Axisymmetry

Elements : 15-Noded

Comments

Mesh

Number of elements : 161

Number of nodes : 1383

Number of stress points : 1932

Average element size :  $1.93 \times 10^0$  m

OK

Figure A.4 General Information for the pile of White Nile bridge area

**Load info**

Distributed loads

Load no.	Load system	Node	X [ $10^{-3}$ m]	Y [m]	qx [kN/m/m]	qy [kN/m/m]
1	A	7	250.000	20.000	0.000	0.000
		27	0.000	20.000	0.000	0.000

Figure A.5 Load information for the pile of White Nile bridge area

pile of white Nile bridge.502

**Soil and Interfaces Info**

Linear Elastic    Mohr-Coulomb

ID	Name	Type	$\gamma_{unsat}$ [kN/m <sup>3</sup> ]	$\gamma_{sat}$ [kN/m <sup>3</sup> ]	$k_x$ [m/s]	$k_y$ [m/s]	$\nu$ [ - ]
1	silty clay	UnDrained	14.8	18.9	0.0000	0.0000	0.35
2	clayleysand	UnDrained	0.0	19.0	0.0000	0.0000	0.30
3	sandy clay	UnDrained	0.0	20.0	0.0000	0.0000	0.30

Copy    Print...    OK

pile of white Nile bridge.502

**Soil and Interfaces Info**

Linear Elastic    Mohr-Coulomb

ID	Name	Type	$\gamma_{unsat}$ [kN/m <sup>3</sup> ]	$\gamma_{sat}$ [kN/m <sup>3</sup> ]	$k_x$ [m/s]	$k_y$ [m/s]	$\nu$ [ - ]
4	pile	Non-porous	25.0	25.0	0.0000	0.0000	0.30

Copy    Print...    OK

Figure A.6 Soil and Interfaces information for the pile of White Nile bridge area

## Appendix A4 pile of Khartoum airport area

The output which represent the plot of the settlement of the pile (top point) versus time and the deform mesh for the pile of Khartoum airport model

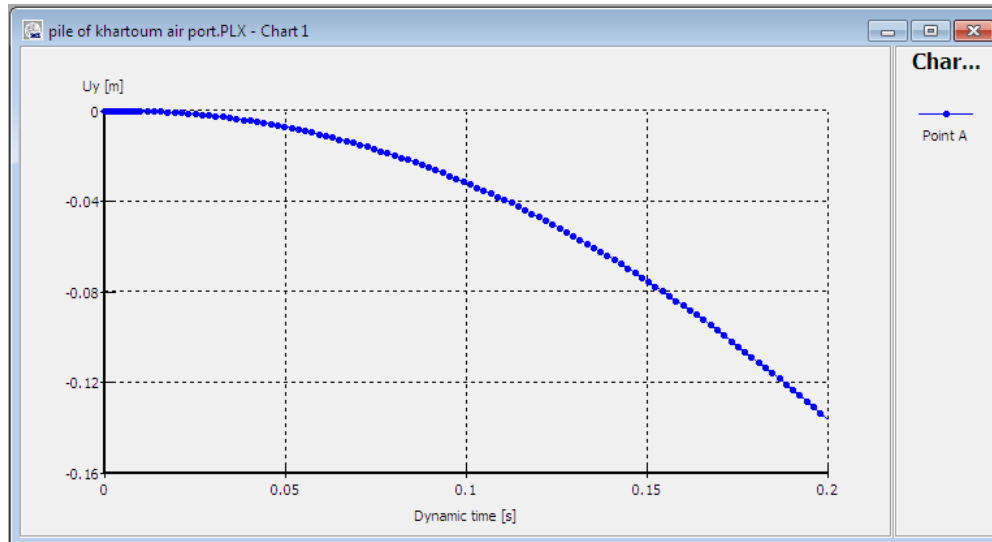


Figure A.7 the displacement of the pile for of Khartoum air port

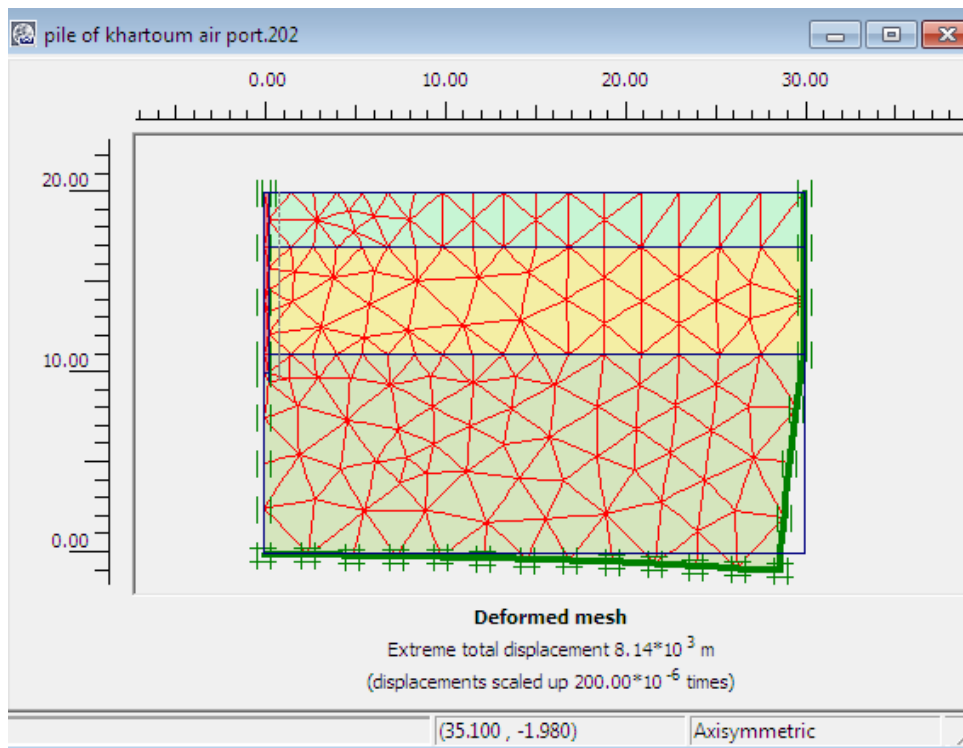


Figure A.8 the deform mesh for of Khartoum air port